



PUBLISHED FOR SISSA BY SPRINGER

RECEIVED: August 1, 2016

REVISED: October 26, 2016

ACCEPTED: November 25, 2016

PUBLISHED: December 16, 2016

Singularity-free next-to-leading order $\Delta S = 1$ renormalization group evolution and ϵ'_K/ϵ_K in the Standard Model and beyond

Teppei Kitahara,^{a,b} Ulrich Nierste^a and Paul Tremper^a

^a*Institute for Theoretical Particle Physics (TTP), Karlsruhe Institute of Technology, Engesserstraße 7, Karlsruhe, D-76128 Germany*

^b*Institute for Nuclear Physics (IKP), Karlsruhe Institute of Technology, Hermann-von-Helmholtz-Platz 1, Eggenstein-Leopoldshafen, D-76344 Germany*

E-mail: tepei.kitahara@kit.edu, Ulrich.Nierste@kit.edu,
paul.tremper@kit.edu

ABSTRACT: The standard analytic solution of the renormalization group (RG) evolution for the $\Delta S = 1$ Wilson coefficients involves several singularities, which complicate analytic solutions. In this paper we derive a singularity-free solution of the next-to-leading order (NLO) RG equations, which greatly facilitates the calculation of ϵ'_K , the measure of direct CP violation in $K \rightarrow \pi\pi$ decays. Using our new RG evolution and the latest lattice results for the hadronic matrix elements, we calculate the ratio ϵ'_K/ϵ_K (with ϵ_K quantifying indirect CP violation) in the Standard Model (SM) at NLO to $\epsilon'_K/\epsilon_K = (1.06 \pm 5.07) \times 10^{-4}$, which is 2.8σ below the experimental value. We also present the evolution matrix in the high-energy regime for calculations of new physics contributions and derive easy-to-use approximate formulae. We find that the RG amplification of new-physics contributions to Wilson coefficients of the electroweak penguin operators is further enhanced by the NLO corrections: if the new contribution is generated at the scale of 1–10 TeV, the RG evolution between the new-physics scale and the electroweak scale enhances these coefficients by 50–100%. Our solution contains a term of order $\alpha_{\text{EM}}^2/\alpha_s^2$, which is numerically unimportant for the SM case but should be included in studies of high-scale new-physics.

KEYWORDS: Renormalization Group, CP violation, Kaon Physics

ARXIV EPRINT: [1607.06727](https://arxiv.org/abs/1607.06727)

Contents

1	Introduction	1
2	Renormalization group evolution of the $\Delta S = 1$ Hamiltonian	3
2.1	Singularities in the evolution matrix	4
2.2	Removing the singularities	6
2.3	Cancellation of spurious parameters	13
2.4	Validation of the logarithmic contribution	16
2.5	Higher orders in α_{EM} and comparison with ref. [22]	16
3	ϵ'_K/ϵ_K in the Standard Model at next-to-leading order	17
4	Beyond the Standard Model	24
4.1	Preliminaries	24
4.2	Counting of orders	26
4.3	Evolution matrices at the TeV scale	27
5	Conclusions and discussion	28
A	Solutions for the matrices \hat{J}	31
B	Approximation of evolution matrices	38

1 Introduction

The parameter ϵ'_K/ϵ_K is the ratio of the measures of direct and indirect charge-parity (CP) violation in the Kaon system. While indirect CP violation is a per-mille effect in the Standard Model (SM), ϵ'_K is smaller by another three orders of magnitude than ϵ_K , with $|\epsilon'_K| \sim \mathcal{O}(10^{-6})$. A strong suppression by the Glashow-Iliopoulos-Maiani (GIM) mechanism and an accidental cancellation of leading contributions in the Standard Model makes ϵ'_K/ϵ_K highly sensitive to new physics. The first element of the SM prediction for ϵ'_K is the calculation of initial conditions for Wilson coefficients and their renormalization group evolution from the electroweak scale (of the order of W and top mass) down to the hadronic scale of order 1 GeV, at which hadronic matrix elements are calculated. These steps purely involve perturbative methods and have been carried out to leading order (LO) in the strong coupling constant α_s in refs. [1–4]. The next-to-leading order (NLO) involves the electromagnetic coupling $\alpha_{\text{EM}} \simeq 1/128$ [5–8], the next higher order in α_s [9–11], and order $\alpha_{\text{EM}}\alpha_s$ [11–13]. In terms of isospin amplitudes ϵ'_K is given by (see e.g. ref. [14])

$$\frac{\epsilon'_K}{\epsilon_K} = \frac{\omega_+}{\sqrt{2}|\epsilon_K|\text{Re} A_0} \left(\frac{1}{\omega_+} \text{Im} A_2 - (1 - \hat{\Omega}_{\text{eff}}) \text{Im} A_0 \right), \quad (1.1)$$

where $A_I \equiv \langle (\pi\pi)_I | \mathcal{H}_{\text{eff}}^{|\Delta S|=1} | K^0 \rangle$ are isospin amplitudes and $\omega_+ = (4.53 \pm 0.02) \times 10^{-2}$ (see refs. [14, 15] for the precise definition), $|\epsilon_K| = (2.228 \pm 0.011) \cdot 10^{-3}$, and $\text{Re } A_0 = (3.3201 \pm 0.0018) \times 10^{-7} \text{ GeV}$ are taken from experiment. $\hat{\Omega}_{\text{eff}} = (14.8 \pm 8.0) \times 10^{-2}$ parameterizes isospin-violating contributions [15, 16].

The $|\Delta S| = 1$ nonleptonic effective Hamiltonian for weak decays in the Standard Model is given by [13]

$$\mathcal{H}_{\text{eff}}^{|\Delta S|=1} = \frac{G_F}{\sqrt{2}} \lambda_u \sum_{i=1}^{10} Q_i(\mu) \left((1 - \tau) z_i(\mu) + \tau v_i(\mu) \right) + \text{H.c.} \quad (1.2)$$

$$\equiv \frac{G_F}{\sqrt{2}} \lambda_u \sum_{i=1}^{10} Q_i(\mu) (z_i(\mu) + \tau y_i(\mu)) + \text{H.c.}, \quad (1.3)$$

where $\lambda_u = V_{us}^* V_{ud}$ and $\tau = -V_{ts}^* V_{td} / (V_{us}^* V_{ud})$. The operator basis Q_i comprises ten operators which are defined in ref. [13]; the current-current operators Q_1 and Q_2

$$Q_1 = (\bar{s}_\alpha u_\beta)_{V-A} (\bar{u}_\beta d_\alpha)_{V-A}, \quad Q_2 = (\bar{s}u)_{V-A} (\bar{u}d)_{V-A}, \quad (1.4)$$

the QCD-penguin operators Q_3 to Q_6

$$Q_3 = (\bar{s}d)_{V-A} \sum_q (\bar{q}q)_{V-A}, \quad Q_4 = (\bar{s}_\alpha d_\beta)_{V-A} \sum_q (\bar{q}_\beta q_\alpha)_{V-A}, \quad (1.5)$$

$$Q_5 = (\bar{s}d)_{V-A} \sum_q (\bar{q}q)_{V+A}, \quad Q_6 = (\bar{s}_\alpha d_\beta)_{V-A} \sum_q (\bar{q}_\beta q_\alpha)_{V+A}, \quad (1.6)$$

and the QED-penguin operators Q_7 to Q_{10}

$$Q_7 = \frac{3}{2} (\bar{s}d)_{V-A} \sum_q e_q (\bar{q}q)_{V+A}, \quad Q_8 = \frac{3}{2} (\bar{s}_\alpha d_\beta)_{V-A} \sum_q e_q (\bar{q}_\beta q_\alpha)_{V+A}, \quad (1.7)$$

$$Q_9 = \frac{3}{2} (\bar{s}d)_{V-A} \sum_q e_q (\bar{q}q)_{V-A}, \quad Q_{10} = \frac{3}{2} (\bar{s}_\alpha d_\beta)_{V-A} \sum_q e_q (\bar{q}_\beta q_\alpha)_{V-A}, \quad (1.8)$$

where $V \mp A$ represents $\gamma_\mu(1 \mp \gamma_5)$, α and β denote color indices, and e_q is the electric charge of the quark q . The corresponding Wilson coefficients z_i and v_i (or y_i) serve as effective couplings to these effective operators.

By virtue of the framework of effective theories, the parameter μ splits short distance from long distance scales, effectively separating the perturbative high energy regime from the non-perturbative realm of low energy QCD. Taking up the perturbative part of the calculation, the Wilson coefficients have been determined through matching calculations up to next-to-leading order at the scale M_W [13]. The calculation of the hadronic matrix elements, being non-perturbative quantities, is a major challenge and has recently been performed on the lattice with unprecedented accuracy [17–20].

The combination of these calculations into a prediction for ϵ'_K/ϵ_K requires a treatment within renormalization group (RG) improved perturbation theory to sum up large logarithms. However, it is known that the analytic determination of the required evolution

matrix at the next-to-leading order suffers from singularities appearing in intermediate steps of the calculation, which make a computational evaluation highly laborious and complicated. The standard way to solve the NLO RG equations requires the diagonalization of the LO anomalous dimension matrix $\hat{\gamma}_s^{(0)}$ and the NLO correction involves fractions whose denominators contain the differences of eigenvalues of $\hat{\gamma}_s^{(0)}$. Some of these denominators vanish and are usually regulated in the numerical evaluation [11, 21]. In ref. [22] an analytic solution for the RG equations which is free of singularities is presented. This solution involves the diagonalization of $\hat{\gamma}_s^{(0)}$ and gives explicit prescriptions to handle the different cases in which the formulae of refs. [11, 21] develop singularities.

In this paper, we present a new singularity-free solution which permits an easy and convenient numerical implementation. Instead of singularities our analytic formula has undetermined parameters. However, we will show that these spurious parameters cancel and leave the evolution matrix unambiguous. Unlike the solution of ref. [22] our new formula requires neither the diagonalization of $\hat{\gamma}_s^{(0)}$ nor a distinct treatment of the part of the RG evolution which involves the spurious singularities. Using our new RG evolution and the latest lattice results [17–20], we calculate the ϵ'_K/ϵ_K in the Standard Model at next-to-leading order to find a value which is below the experimentally measured quantity by 2.8σ .

The second objective of this paper is the derivation of a useful formula for the calculation of new physics contributions to ϵ'_K/ϵ_K , in which we evaluate the evolution matrices for scales far above the electroweak scale. To this end we identify a contribution of order $\alpha_{\text{EM}}^2/\alpha_s^2$ in the evolution matrix which can become relevant for studies of TeV-scale new physics, because α_s decreases with increasing scale. We observe an approximately logarithmic behavior of the evolution matrix as a function of the energy scale above the electroweak scale.

This paper is organized as follows. In section 2, we briefly review the RG evolution of the $|\Delta S| = 1$ effective Hamiltonian at the next-to-leading order. We give a detailed analysis of the evolution matrix and its singularities and provide a new analytic solution without singularities. Then we evaluate ϵ'_K/ϵ_K in the Standard Model at the next-to-leading order in section 3. In section 4, we work out the evolution matrices in the high-energy regime explicitly for calculations of new physics contributions. The last section is devoted to conclusions and discussion.

2 Renormalization group evolution of the $\Delta S = 1$ Hamiltonian

In this section, we review the singularities in the RG evolution of the $|\Delta S| = 1$ effective Hamiltonian at the next-to-leading order. Then we generalize the analytic ansatz of the RG evolution given in the literature and present a solution, which is finite at all stages of the calculation. Our solution contains free parameters, which we show to cancel from the evolution matrix, and compare our singularity-free solution with the standard results from the literature.

2.1 Singularities in the evolution matrix

The evolution of the Wilson coefficients v_i and z_i from the W boson mass and the charm mass respectively to the hadronic scale μ are given by

$$\vec{v}(\mu) = \hat{U}_3(\mu, \mu_c) \hat{M}_c(\mu_c) \hat{U}_4(\mu_c, m_b) \hat{M}_b(m_b) \hat{U}_5(m_b, M_W) \vec{v}(M_W), \quad (2.1)$$

$$\vec{z}(\mu) = \hat{U}_3(\mu, \mu_c) \vec{z}(\mu_c), \quad (2.2)$$

where $\hat{U}_f(\mu_1, \mu_2)$ is the RG evolution matrix from μ_2 down to μ_1 and f is the number of the active flavors between these two energy scales. The matrices $\hat{M}_{c,b}$ represent matching matrices between effective theories with different numbers of flavor and are given in ref. [13]. Although the effect of the running of α_{EM} is numerically negligible for ϵ'_K/ϵ_K in the Standard Model [13], we consider this effect to cover new-physics scenarios with largely separate scales.

The general form of the evolution matrix is given by [23, 24],

$$\hat{U}_f(\mu_1, \mu_2) = T_{g_s} \exp \int_{g_s(\mu_2)}^{g_s(\mu_1)} dg'_s \frac{\hat{\gamma}^T(g'_s)}{\beta(g'_s)}, \quad (2.3)$$

with the g_s -ordering operator T_{g_s} and the anomalous dimension matrix $\hat{\gamma}$ and the QCD β function. The expansions of the latter two quantities and α_{EM} up to NLO read:

$$\hat{\gamma}(g_s(\mu)) = \frac{\alpha_s(\mu)}{4\pi} \hat{\gamma}_s^{(0)} + \frac{\alpha_{\text{EM}}(\mu)}{4\pi} \hat{\gamma}_e^{(0)} + \frac{\alpha_s^2(\mu)}{(4\pi)^2} \hat{\gamma}_s^{(1)} + \frac{\alpha_{\text{EM}}(\mu)\alpha_s(\mu)}{(4\pi)^2} \hat{\gamma}_{se}^{(1)}, \quad (2.4)$$

$$\beta(g_s(\mu)) = -g_s(\mu) \left(\frac{\alpha_s(\mu)}{4\pi} \beta_0 + \frac{\alpha_s^2(\mu)}{(4\pi)^2} \beta_1 + \frac{\alpha_s(\mu)\alpha_{\text{EM}}(\mu)}{(4\pi)^2} \beta_1^{se} \right), \quad (2.5)$$

$$\alpha_{\text{EM}}(\mu) = \alpha_{\text{EM}}(M) \left\{ 1 + \frac{\alpha_{\text{EM}}(M)}{\alpha_s(\mu)} \frac{\beta_0^e}{\beta_0} \left(1 - \frac{\alpha_s(\mu)}{\alpha_s(M)} \right) \right\}^{-1}, \quad (2.6)$$

where $\beta_0 = 11 - 2f/3$, $\beta_1 = 102 - 38f/3$, $\beta_1^{se} = -8/9(u + d/4)$, and $\beta_0^e = -4/3(4u/3 + d/3 + \ell)$ are the leading and next-to-leading coefficients of the QCD and QED beta functions, and u, d, ℓ are the numbers of the active up-type-quark, down-type-quark, and charged-lepton flavors ($f = u + d$). $\hat{\gamma}_s^{(0)}$ is the LO QCD anomalous dimension matrix, and the NLO corrections consist of the three remaining matrices, $\hat{\gamma}_e^{(0)}$, $\hat{\gamma}_s^{(1)}$, and $\hat{\gamma}_{se}^{(1)}$, which are the leading QED, next-to-leading QCD, and combined QCD-QED anomalous dimension matrices, respectively.

The ansatz for the NLO evolution matrix (with $\mu_1 < \mu_2$) is given by [11, 21]

$$\hat{U}_f(\mu_1, \mu_2) = \hat{K}(\mu_1) \hat{U}_0(\mu_1, \mu_2) \hat{K}'(\mu_2), \quad (2.7)$$

where

$$\hat{K}(\mu_1) = \left(\hat{1} + \frac{\alpha_{\text{EM}}}{4\pi} \hat{J}_{se} \right) \left(\hat{1} + \frac{\alpha_s(\mu_1)}{4\pi} \hat{J}_s \right) \left(\hat{1} + \frac{\alpha_{\text{EM}}}{\alpha_s(\mu_1)} \hat{J}_e \right), \quad (2.8)$$

$$\hat{K}'(\mu_2) = \left(\hat{1} - \frac{\alpha_{\text{EM}}}{\alpha_s(\mu_2)} \hat{J}_e \right) \left(\hat{1} - \frac{\alpha_s(\mu_2)}{4\pi} \hat{J}_s \right) \left(\hat{1} - \frac{\alpha_{\text{EM}}}{4\pi} \hat{J}_{se} \right), \quad (2.9)$$

and the LO evolution matrix

$$\hat{U}_0(\mu_1, \mu_2) = \hat{U}_0(\alpha_s(\mu_1), \alpha_s(\mu_2)) = \exp \left[\frac{\hat{\gamma}_s^{(0)T}}{2\beta_0} \ln \frac{\alpha_s(\mu_2)}{\alpha_s(\mu_1)} \right], \quad (2.10)$$

where the QED contributions to the beta functions (β_1^{se} , β_0^e) are discarded in this subsection 2.1.

The matrices $\hat{K}(\mu_1)$ and $\hat{K}'(\mu_2)$ encode the NLO corrections and depend on the number of active flavors through the beta function and the anomalous dimension matrices. The matrices \hat{J}_e , \hat{J}_s and \hat{J}_{se} govern the leading electromagnetic, next-to-leading strong, and next-to-leading combined strong-electromagnetic contributions to the RG evolution.

Differentiating eqs. (2.7) and (2.3) with respect to $g_s(\mu_1)$ yields the following differential equation for $\hat{K}(g_s(\mu_1))$ [9, 23],

$$\frac{\partial}{\partial g_s(\mu_1)} \hat{K}(g_s(\mu_1)) - \frac{1}{g_s(\mu_1)} \hat{K}(g_s(\mu_1)) \frac{\hat{\gamma}_s^{(0)T}}{\beta_0} = \frac{\hat{\gamma}^T(g_s(\mu_1))}{\beta(g_s(\mu_1))} \hat{K}(g_s(\mu_1)). \quad (2.11)$$

The traditional ansatz in the literature is to take \hat{J}_e , \hat{J}_s and \hat{J}_{se} as constant matrices for any fixed number of flavors. The differential equation (2.11) then implies the following equations for the matrices \hat{J}_e , \hat{J}_s and \hat{J}_{se} [11],

$$\hat{J}_s - \left[\hat{J}_s, \frac{\hat{\gamma}_s^{(0)T}}{2\beta_0} \right] = \frac{\beta_1}{\beta_0} \frac{\hat{\gamma}_s^{(0)T}}{2\beta_0} - \frac{\hat{\gamma}_s^{(1)T}}{2\beta_0}, \quad (2.12)$$

$$\hat{J}_e + \left[\hat{J}_e, \frac{\hat{\gamma}_s^{(0)T}}{2\beta_0} \right] = \frac{\hat{\gamma}_e^{(0)T}}{2\beta_0}, \quad (2.13)$$

$$\left[\hat{J}_{se}, \frac{\hat{\gamma}_s^{(0)T}}{2\beta_0} \right] = \frac{\hat{\gamma}_{se}^{(1)T}}{2\beta_0} + \left[\frac{\hat{\gamma}_e^{(0)T}}{2\beta_0}, \hat{J}_s \right] - \frac{\beta_1}{\beta_0} \frac{\hat{\gamma}_e^{(0)T}}{2\beta_0}. \quad (2.14)$$

It is well known, however, that eqs. (2.12) and (2.13) develop singularities in the case of three flavors. Furthermore, eq. (2.14) is even singular for any number of flavors.

We now show how these singularities arise. For this purpose, it is instructional to transform eqs. (2.12)–(2.14) into the diagonal basis of $\hat{\gamma}_s^{(0)T}$. This is a common procedure in the literature since it allows to isolate the singularities and remove them “by hand”. We stress that this is only for the purpose of a better understanding of the origin of these singularities. A numerical evaluation of our solution does not require the diagonalisation of $\hat{\gamma}_s^{(0)T}$.

Upon transforming eqs. (2.12)–(2.14) into the basis where $\hat{\gamma}_{s,D}^{(0)T} = \hat{V}^{-1} \hat{\gamma}_s^{(0)T} \hat{V}$ is diagonal, the solutions of eqs. (2.12) and (2.13) take the form

$$\left(\hat{V}^{-1} \hat{J}_{s,e} \hat{V} \right)_{ij} = \frac{\dots}{2\beta_0 \mp \left((\hat{\gamma}_{s,D}^{(0)T})_{jj} - (\hat{\gamma}_{s,D}^{(0)T})_{ii} \right)}. \quad (2.15)$$

We find singular solutions if the difference of two eigenvalues of $\hat{\gamma}_s^{(0)T}$ is equal to $2\beta_0$, which is the case for three flavors: $\hat{\gamma}_{s,D}^{(0)T}$ has the elements 2 and -16 and $2\beta_0^{f=3} = 18$, so that

one denominator in eq. (2.15) vanishes with a generally non-zero numerator. When we transform eq. (2.14) into the same basis

$$\left(\hat{V}^{-1}\hat{J}_{se}\hat{V}\right)_{ij} = \frac{\dots}{(\hat{\gamma}_{s,D}^{(0)T})_{jj} - (\hat{\gamma}_{s,D}^{(0)T})_{ii}}, \quad (2.16)$$

we find singular results for $i = j$ and also for degenerate eigenvalues.

Nonetheless, once all relevant terms have been joined together, all these singularities cancel and the evolution matrix $\hat{U}_f(\mu_1, \mu_2)$ becomes finite [11]. This procedure, however, requires taking care of each singularity by hand by adopting the aforementioned diagonal basis, then regularizing the singularities and keeping track of them until the end of the calculation. Indeed, Buras et al. have regulated some of the singularities by a logarithmic term [13]. Subsequently, Adams and Lee have proposed a systematical solution for all singularities [25], which, however, still requires the adoption of a certain diagonal basis. The freedom of choosing the order of the eigenvalues on the diagonal of $\hat{\gamma}_{s,D}^{(0)T}$ involves an ambiguity. This can pose a problem in computational implementations, since it is absolutely necessary to use the same diagonal basis as Adams and Lee do, which is not the one which orders eigenvalues by their numerical value. The solution in ref. [22] follows the same line, after diagonalizing $\hat{\gamma}_{s,D}^{(0)T}$ several different cases must be considered: whenever two eigenvalues differ by an integer multiple of $2\beta_0$ a special implementation is required. In the next subsection we propose a solution which does not rely on a specific basis and permits a much faster, easier and, in particular, more stable computational algorithm.

2.2 Removing the singularities

In order to eliminate the singularities, we generalize the Roma group's ansatz [11, 21] by adding a logarithmic scale dependence to the \hat{J} matrices used in eqs. (2.8), (2.9) in the following way

$$\begin{aligned} \hat{J}_s &\rightarrow \hat{J}_s(\alpha_s(\mu)) = \hat{J}_{s,0} + \hat{J}_{s,1} \ln \alpha_s(\mu), \\ \hat{J}_e &\rightarrow \hat{J}_e(\alpha_s(\mu)) = \hat{J}_{e,0} + \hat{J}_{e,1} \ln \alpha_s(\mu), \\ \hat{J}_{se} &\rightarrow \hat{J}_{se}(\alpha_s(\mu)) = \hat{J}_{se,0} + \hat{J}_{se,1} \ln \alpha_s(\mu) + \hat{J}_{se,2} \ln^2 \alpha_s(\mu). \end{aligned} \quad (2.17)$$

In addition, we extend eqs. (2.8), (2.9) as follows:

$$\begin{aligned} \hat{K}(\mu_1, \mu_2) &= \left(\hat{1} + \frac{\alpha_{\text{EM}}}{4\pi} \hat{J}_{se}(\alpha_s(\mu_1))\right) \left(\hat{1} + \frac{\alpha_s(\mu_1)}{4\pi} \hat{J}_s(\alpha_s(\mu_1))\right) \\ &\times \left(\hat{1} + \frac{\alpha_{\text{EM}}}{\alpha_s(\mu_1)} \hat{J}_e(\alpha_s(\mu_1))\right. \\ &\quad \left.+ \left(\frac{\alpha_{\text{EM}}}{\alpha_s(\mu_1)}\right)^2 \left(\hat{J}_{ee}(\alpha_s(\mu_1)) - \frac{\beta_0^e}{\beta_0} \left(1 - \frac{\alpha_s(\mu_1)}{\alpha_s(\mu_2)}\right) \hat{J}_e(\alpha_s(\mu_1))\right)\right), \end{aligned} \quad (2.18)$$

$$\begin{aligned} \hat{K}'(\mu_2) &= \left(\hat{1} - \frac{\alpha_{\text{EM}}}{\alpha_s(\mu_2)} \hat{J}_e(\alpha_s(\mu_2)) - \left(\frac{\alpha_{\text{EM}}}{\alpha_s(\mu_2)}\right)^2 \left(\hat{J}_{ee}(\alpha_s(\mu_2)) - \left(\hat{J}_e(\alpha_s(\mu_2))\right)^2\right)\right) \\ &\times \left(\hat{1} - \frac{\alpha_s(\mu_2)}{4\pi} \hat{J}_s(\alpha_s(\mu_2))\right) \left(\hat{1} - \frac{\alpha_{\text{EM}}}{4\pi} \hat{J}_{se}(\alpha_s(\mu_2))\right), \end{aligned} \quad (2.19)$$

which somewhat resembles the NNLO QCD result of ref. [26]. Here we use the abbreviation $\alpha_{\text{EM}} \equiv \alpha_{\text{EM}}(\mu_2)$ and

$$\hat{J}_{ee}(\alpha_s(\mu)) = \hat{J}_{ee,0} + \hat{J}_{ee,1} \ln \alpha_s(\mu). \quad (2.20)$$

We systematically include $\mathcal{O}(\alpha_{\text{EM}}^2/\alpha_s^2)$ corrections in the RG evolution. This contribution has not been considered in the literature. Although appearing as $\mathcal{O}(\alpha_{\text{EM}}^2)$, these terms can become sizable at high energies because of the awkward $1/\alpha_s^2$ dependence, making them numerically comparable to $\mathcal{O}(\alpha_s)$. We note that this contribution does not receive contributions from higher orders of the anomalous dimension matrix in eq. (2.4), but only appears at the next-to-leading order.

With these generalizations we can now solve the differential equation in eq. (2.11). Inserting our ansatz into eq. (2.11) we obtain the following nine matrix equations for the nine constant matrices \hat{J} :

$$\hat{J}_{s,1} - \left[\hat{J}_{s,1}, \frac{\hat{\gamma}_s^{(0)T}}{2\beta_0} \right] = 0, \quad (2.21)$$

$$\hat{J}_{s,0} - \left[\hat{J}_{s,0}, \frac{\hat{\gamma}_s^{(0)T}}{2\beta_0} \right] = \frac{\beta_1}{\beta_0} \frac{\hat{\gamma}_s^{(0)T}}{2\beta_0} - \frac{\hat{\gamma}_s^{(1)T}}{2\beta_0} - \hat{J}_{s,1}, \quad (2.22)$$

$$\hat{J}_{e,1} + \left[\hat{J}_{e,1}, \frac{\hat{\gamma}_s^{(0)T}}{2\beta_0} \right] = 0, \quad (2.23)$$

$$\hat{J}_{e,0} + \left[\hat{J}_{e,0}, \frac{\hat{\gamma}_s^{(0)T}}{2\beta_0} \right] = \frac{\hat{\gamma}_e^{(0)T}}{2\beta_0} + \hat{J}_{e,1}, \quad (2.24)$$

$$\left[\hat{J}_{se,2}, \frac{\hat{\gamma}_s^{(0)T}}{2\beta_0} \right] = 0, \quad (2.25)$$

$$\left[\hat{J}_{se,1}, \frac{\hat{\gamma}_s^{(0)T}}{2\beta_0} \right] = \left[\frac{\hat{\gamma}_e^{(0)T}}{2\beta_0}, \hat{J}_{s,1} \right] + 2\hat{J}_{se,2}, \quad (2.26)$$

$$\left[\hat{J}_{se,0}, \frac{\hat{\gamma}_s^{(0)T}}{2\beta_0} \right] = \frac{\hat{\gamma}_{se}^{(1)T}}{2\beta_0} + \left[\frac{\hat{\gamma}_e^{(0)T}}{2\beta_0}, \hat{J}_{s,0} \right] - \frac{\beta_1}{\beta_0} \frac{\hat{\gamma}_e^{(0)T}}{2\beta_0} - \frac{\beta_1^{se}}{\beta_0} \frac{\hat{\gamma}_s^{(0)T}}{2\beta_0} + \hat{J}_{se,1}, \quad (2.27)$$

$$\hat{J}_{ee,1} + \left[\hat{J}_{ee,1}, \frac{\hat{\gamma}_s^{(0)T}}{4\beta_0} \right] = \frac{\hat{\gamma}_e^{(0)T}}{4\beta_0} \hat{J}_{e,1} + \frac{1}{2} \frac{\beta_0^e}{\beta_0} \hat{J}_{e,1}, \quad (2.28)$$

$$\hat{J}_{ee,0} + \left[\hat{J}_{ee,0}, \frac{\hat{\gamma}_s^{(0)T}}{4\beta_0} \right] = \frac{\hat{\gamma}_e^{(0)T}}{4\beta_0} \hat{J}_{e,0} + \frac{1}{2} \frac{\beta_0^e}{\beta_0} \hat{J}_{e,0} + \frac{1}{2} \hat{J}_{ee,1}. \quad (2.29)$$

These equations yield finite solutions for \hat{J} . As an effect of the constant matrices $\hat{J}_{s(e,se),1}$, the analytic singularities of eqs. (2.12)–(2.14) do not occur, because for the problematic matrix elements now both sides of the equations are zero. We stress that one can solve eqs. (2.21) to (2.29) without diagonalizing $\hat{\gamma}_s^{(0)T}$; these equations are mere systems of linear equations for the 100 elements of $\hat{J}_{s,e,ee,0,1}$ and $\hat{J}_{se,0,1,2}$ each, which are quickly

solved by computer algebra programs [27]. However, there are multiple solutions in some of the inhomogeneous equations, because the corresponding homogeneous equations have a non-trivial null space. As a consequence, these solutions for \hat{J} depend on arbitrary parameters, e.g. there are 16 undetermined components in the case of three active flavors. These parameters, however, do not produce any ambiguity in physical results. In the next subsection, we will show that they completely drop out after combining terms of the same order and the evolution matrix in eq. (2.7) does not depend on these parameters. Therefore, one can set them to arbitrary values from the beginning. In our calculation of ϵ'_K/ϵ_K we kept the parameters arbitrary as a crosscheck of the consistency of our calculation.

The procedure to determine the evolution matrix from μ_2 to μ_1 requires algebraically solving the matrix equations (2.21)–(2.29) for a given number of active flavors and inserting the solutions into the full evolution matrix in eq. (2.7). We use 10×10 anomalous dimension matrices $\hat{\gamma}_s^{(0)}$, $\hat{\gamma}_e^{(0)}$, $\hat{\gamma}_s^{(1)}$ and $\hat{\gamma}_{se}^{(1)}$ [10–12, 24]. The solutions for the matrices \hat{J} in the case of three active flavors (with two active leptons) in naive dimensional regularization (NDR) scheme with $\overline{\text{MS}}$ subtraction, are given as follows:

$$\hat{J}_{s,0} = \begin{pmatrix} -55/324 & 223/108 & 0 & 0 & 0 & 0 & 0 & 0 & 0 & 0 \\ 223/108 & -55/324 & 0 & 0 & 0 & 0 & 0 & 0 & 0 & 0 \\ -0.7392 & -0.3061 & -2.999 & -0.6652 & 1.457 & 0.2171 & 0 & 0 & 0.3061 & 0.7392 \\ 0.3814 & -0.1853 & 2.838 & 1.037 & -0.05711 & -0.004122 & 0 & 0 & 0.1853 & -0.3814 \\ 0.3990 & 0.3264 & 1.850 & 1.444 & -2.514 & 2.750 & 0 & 0 & -0.3264 & -0.3990 \\ -1.181 & -1.776 & -7.095 & -6.691 & 0.6263 & 4.528 & 0 & 0 & 1.776 & 1.181 \\ 0 & 0 & 0 & 0 & 0 & 0 & -679/648 & 67/24 & 0 & 0 \\ 0 & 0 & 0 & 0 & 0 & 0 & t_s & 3749/648 & 0 & 0 \\ 0 & 0 & 0 & 0 & 0 & 0 & 0 & 0 & -55/324 & 223/108 \\ 0 & 0 & 0 & 0 & 0 & 0 & 0 & 0 & 223/108 & -55/324 \end{pmatrix}, \quad (2.30)$$

$$\hat{J}_{s,1} = \begin{pmatrix} 0 & 0 & 0 & 0 & 0 & 0 & 0 & 0 & 0 & 0 \\ 0 & 0 & 0 & 0 & 0 & 0 & 0 & 0 & 0 & 0 \\ 0 & 0 & 0 & 0 & 0 & 0 & 0 & 0 & 0 & 0 \\ 0 & 0 & 0 & 0 & 0 & 0 & 0 & 0 & 0 & 0 \\ 0 & 0 & 0 & 0 & 0 & 0 & 0 & 0 & 0 & 0 \\ 0 & 0 & 0 & 0 & 0 & 0 & 0 & 0 & 0 & 0 \\ 0 & 0 & 0 & 0 & 0 & 0 & 0 & 0 & 0 & 0 \\ 0 & 0 & 0 & 0 & 0 & 0 & 0 & 0 & 0 & 0 \\ 0 & 0 & 0 & 0 & 0 & 0 & -10/27 & 0 & 0 & 0 \\ 0 & 0 & 0 & 0 & 0 & 0 & 0 & 0 & 0 & 0 \\ 0 & 0 & 0 & 0 & 0 & 0 & 0 & 0 & 0 & 0 \end{pmatrix}, \quad (2.31)$$

$$\hat{J}_{se,0} = \begin{pmatrix} 3/8 & 9/8 & 0 & 0 & 0 & 0 & 0 & 0 & 0 & 0 \\ -9/8 & -3/8 & 0 & 0 & 0 & 0 & 0 & 0 & 0 & 0 \\ -26.08 & 20.94 & -25.20 & 22.07 & 4.847 & 8.717 & 16.02 & 0.00499 & -26.20 & 20.63 \\ 21.87 & -25.07 & 31.46 & -15.23 & -5.751 & -8.314 & 7.459 & 0.05014 & 16.21 & -30.05 \\ 2.409 & 2.535 & -1.122 & -0.9967 & 0.06192 & -0.1911 & 2t_s/5+142.6 & 0.02577 & 4.175 & 4.300 \\ -1.581 & -1.594 & 0.7172 & 0.7036 & 0.1306 & 0.1116 & -8t_s/135-51.94 & -2.417 & -2.729 & -2.743 \\ -15.68 & -11.02 & -59.91 & -55.25 & -309.3 & 8.235 & 0.08482 & 0.2545 & 7.761 & 11.53 \\ -2t_s/15+5.611 & 2t_s/135+2.955 & -2t_s/135+19.78 & 2t_s/15+17.12 & -59t_s/270+102.8 & -19t_s/90-3.773 & -28t_s/243+0.4857 & -0.08482 & -26t_s/135-1.473 & -2t_s/45-4.129 \\ 27.12 & -19.23 & 45.81 & -0.03029 & -8.332 & -7.461 & -8t_s/45+1.621 & -0.3044 & 18.81 & -27.48 \\ -21.04 & 26.43 & -13.67 & 34.30 & 2.682 & 10.09 & -4t_s/15+3.035 & 0.8012 & -26.07 & 21.45 \end{pmatrix}$$

$$+ \hat{V} \begin{pmatrix} t_{se1} & 0 & 0 & 0 & 0 & 0 & 0 & 0 & 0 & 0 \\ 0 & t_{se2} & 0 & 0 & 0 & 0 & 0 & 0 & 0 & 0 \\ 0 & 0 & t_{se3} & t_{se4} & 0 & 0 & 0 & 0 & 0 & 0 \\ 0 & 0 & t_{se5} & t_{se6} & 0 & 0 & 0 & 0 & 0 & 0 \\ 0 & 0 & 0 & 0 & t_{se7} & 0 & 0 & 0 & 0 & 0 \\ 0 & 0 & 0 & 0 & 0 & t_{se8} & 0 & 0 & 0 & 0 \\ 0 & 0 & 0 & 0 & 0 & 0 & t_{se9} & t_{se10} & 0 & 0 \\ 0 & 0 & 0 & 0 & 0 & 0 & t_{se11} & t_{se12} & 0 & 0 \\ 0 & 0 & 0 & 0 & 0 & 0 & 0 & 0 & t_{se13} & 0 \\ 0 & 0 & 0 & 0 & 0 & 0 & 0 & 0 & 0 & t_{se14} \end{pmatrix} \hat{V}^{-1}, \quad (2.34)$$

$$\hat{J}_{se,1} = \begin{pmatrix} -1.485 & -0.2623 & 0 & 0 & 0 & 0 & 0 & 0 & 0 & 0 \\ -0.2623 & -1.485 & 0 & 0 & 0 & 0 & 0 & 0 & 0 & 0 \\ -0.3914 & 0.9178 & -0.5086 & 0.8458 & 0.1026 & 0.1994 & 0 & 0 & -1.075 & 0.8226 \\ 0.9599 & -0.2650 & 1.225 & -0.04511 & -0.1655 & -0.1095 & 0 & 0 & 0.6962 & -1.117 \\ -0.002595 & -0.04387 & -0.09552 & -0.1368 & 0.1728 & -0.03447 & -0.1481 & 0 & 0.04387 & 0.002595 \\ 0.05517 & 0.000282 & 0.1661 & 0.1112 & -0.2131 & -0.3630 & 0.02195 & 0 & -0.000282 & -0.05517 \\ 0 & 0 & 0 & 0 & 0 & 0 & -4t_s/81 + 1.985 & 0 & 0 & 0 \\ 0.04938 & -0.005487 & 0.005487 & -0.04938 & 0.08093 & 0.07819 & 8t_s/243 - 0.9268 & 4t_s/81 - 0.9234 & 0.07133 & 0.01646 \\ 0.8624 & -0.3145 & 0 & 0 & 0 & 0 & 0.06584 & 0 & -0.1909 & -0.7342 \\ -0.3145 & 0.8624 & 0 & 0 & 0 & 0 & 0.09877 & 0 & -0.7342 & -0.1909 \end{pmatrix}, \quad (2.35)$$

$$\hat{J}_{se,2} = \begin{pmatrix} 0 & 0 & 0 & 0 \\ 0 & 0 & 0 & 0 \\ 0 & 0 & 0 & 0 \\ 0 & 0 & 0 & 0 \\ 0 & 0 & 0 & 0 \\ 0 & 0 & 0 & 0 \\ 0 & 20/2187 & 0 & 0 \\ 0 & -40/6561 & -20/2187 & 0 \\ 0 & 0 & 0 & 0 \\ 0 & 0 & 0 & 0 \end{pmatrix}, \quad (2.36)$$

$$\hat{J}_{ee,0} = \begin{pmatrix} 40/729 & 0 & 0 & 0 & 0 & 0 & 0 & 0 & 0 & 0 \\ 0 & 40/729 & 0 & 0 & 0 & 0 & 0 & 0 & 0 & 0 \\ -0.002519 & -0.003958 & 0.000955 & -0.005971 & 0.03395 & 0.09227 & 12t_e/27083+0.001188 & 36t_e/27083+0.01576 & 0.02318 & -0.002951 \\ 0.000504 & -0.001464 & -0.006771 & -0.003253 & 0.03333 & 0.09097 & -180t_e/27083+0.01104 & -540t_e/27083+0.03144 & 0.004142 & 0.02686 \\ 0.005995 & -0.003625 & 0.002241 & -0.007379 & 0.01478 & 0.02625 & 8026t_e/104463-0.1123 & 8026t_e/34821-0.2909 & 0.007872 & -0.001747 \\ -0.001130 & 0.002451 & -0.001997 & 0.001584 & -0.003039 & -0.002932 & -9178t_e/313389+0.03477 & -9178t_e/104463+0.08429 & -0.000697 & 0.002884 \\ -0.02801 & 0.01209 & -0.01239 & 0.02771 & -0.09800 & -0.1928 & -94t_e/243+0.06658 & -94t_e/81+0.2660 & -0.03582 & 0.004286 \\ 0.008577 & -0.003761 & 0.004577 & -0.007761 & 0.01725 & 0.01575 & 110t_e/729-0.03402 & 110t_e/243-0.1293 & 0.01058 & -0.001761 \\ -0.02099 & -0.01189 & 0.02183 & -0.01845 & 0.1185 & 0.2984 & 22t_e/189-0.005245 & 22t_e/63+0.02511 & 0.01247 & -0.008604 \\ -0.009687 & -0.01325 & -0.02604 & 0.01978 & 0.1295 & 0.3422 & 2t_e/63+0.03922 & 2t_e/21+0.1510 & -0.001510 & 0.02511 \end{pmatrix}, \quad (2.37)$$

$$\hat{J}_{ee,1} = \begin{pmatrix} 0 & 0 & 0 & 0 \\ 0 & 0 & 0 & 0 \\ 0 & -16/2193723 & -16/731241 & 0 \\ 0 & 80/731241 & 80/243747 & 0 \\ 0 & -32104/25384509 & -32104/8461503 & 0 \\ 0 & 36712/76153527 & 36712/25384509 & 0 \\ 0 & 376/59049 & 376/19683 & 0 \\ 0 & -440/177147 & -440/59049 & 0 \\ 0 & -88/45927 & -88/15309 & 0 \\ 0 & -8/15309 & -8/5103 & 0 \end{pmatrix}, \quad (2.38)$$

where t_s , t_e , and $t_{se1,2,\dots,14}$ are the arbitrary parameters of the matrix equations. Our convention for the matrix \hat{V} is $(\hat{\gamma}_{s,D}^{(0)T})_{1,1} \leq (\hat{\gamma}_{s,D}^{(0)T})_{2,2} \leq \dots \leq (\hat{\gamma}_{s,D}^{(0)T})_{10,10}$. Although eq. (2.34) makes explicit reference to the diagonal basis, the term involving \hat{V} completely drops out from the evolution matrix (see next subsection), and thereby our solution for the latter does not require any matrix diagonalisation. Our eqs. (2.18)–(2.29) hold in any operator basis. Moreover, if an ordinary four-dimensional basis transformation is applied to eqs. (1.4)–(1.8), the corresponding RG matrices \hat{J}_{\dots} can be simply found by transforming those in eqs. (2.30)–(2.38) in the same way as $\hat{\gamma}_s^{(0)T}$. If the basis transformation is D -dimensional, meaning that it involves evanescent operators, the \hat{J}_{\dots} matrices undergo an additional scheme transformation [26, 28]. We collect the solutions for more than three active flavors in appendix A.

Substituting the generalized ansatz of eqs. (2.18), (2.19) into eq. (2.7), we find the full next-to-leading order evolution matrix,

$$\begin{aligned} \hat{U}_f(\alpha_1, \alpha_2) &= \hat{U}_0(\alpha_1, \alpha_2) + \frac{\alpha_1}{4\pi} \hat{U}_{\text{QCD}}(\alpha_1, \alpha_2) + \frac{\alpha_{\text{EM}}}{\alpha_1} \hat{U}_{\text{QED}}(\alpha_1, \alpha_2) \\ &+ \frac{\alpha_{\text{EM}}}{4\pi} \hat{U}_{\text{QCD-QED}}(\alpha_1, \alpha_2) + \left(\frac{\alpha_{\text{EM}}}{\alpha_1} \right)^2 \hat{U}_{\text{QED-QED}}(\alpha_1, \alpha_2) \\ &+ \mathcal{O}\left(\frac{\alpha_{\text{EM}}^2}{\alpha_s}, \alpha_s^2, \alpha_s \alpha_{\text{EM}}, \alpha_{\text{EM}}^2 \right), \end{aligned} \quad (2.39)$$

where we use the abbreviation $\alpha_{1,2} \equiv \alpha_s(\mu_{1,2})$ for $\mu_1 < \mu_2$ and $\alpha_{\text{EM}} \equiv \alpha_{\text{EM}}(\mu_2)$ with

$$\hat{U}_{\text{QCD}}(\alpha_1, \alpha_2) = \hat{J}_s(\alpha_1) \hat{U}_0(\alpha_1, \alpha_2) - \frac{\alpha_2}{\alpha_1} \hat{U}_0(\alpha_1, \alpha_2) \hat{J}_s(\alpha_2), \quad (2.40)$$

$$\hat{U}_{\text{QED}}(\alpha_1, \alpha_2) = \hat{J}_e(\alpha_1) \hat{U}_0(\alpha_1, \alpha_2) - \frac{\alpha_1}{\alpha_2} \hat{U}_0(\alpha_1, \alpha_2) \hat{J}_e(\alpha_2), \quad (2.41)$$

$$\begin{aligned} \hat{U}_{\text{QCD-QED}}(\alpha_1, \alpha_2) &= \hat{J}_{se}(\alpha_1) \hat{U}_0(\alpha_1, \alpha_2) - \hat{U}_0(\alpha_1, \alpha_2) \hat{J}_{se}(\alpha_2) \\ &+ \hat{J}_s(\alpha_1) \hat{U}_{\text{QED}}(\alpha_1, \alpha_2) - \frac{\alpha_2}{\alpha_1} \hat{U}_{\text{QED}}(\alpha_1, \alpha_2) \hat{J}_s(\alpha_2), \end{aligned} \quad (2.42)$$

$$\begin{aligned} \hat{U}_{\text{QED-QED}}(\alpha_1, \alpha_2) &= \hat{J}_{ee}(\alpha_1) \hat{U}_0(\alpha_1, \alpha_2) - \frac{\alpha_1}{\alpha_2} \hat{U}_{\text{QED}}(\alpha_1, \alpha_2) \hat{J}_e(\alpha_2) \\ &- \left(\frac{\alpha_1}{\alpha_2} \right)^2 \hat{U}_0(\alpha_1, \alpha_2) \hat{J}_{ee}(\alpha_2) - \frac{\beta_0^e}{\beta_0} \left(1 - \frac{\alpha_1}{\alpha_2} \right) \hat{J}_e(\alpha_1) \hat{U}_0(\alpha_1, \alpha_2). \end{aligned} \quad (2.43)$$

2.3 Cancellation of spurious parameters

We now present some details of the cancellation of the arbitrary parameters. First, we take a look at the $\mathcal{O}(\alpha_s)$ part of the evolution matrix in eq. (2.39),

$$\begin{aligned} \frac{\alpha_1}{4\pi} \hat{U}_{\text{QCD}}(\alpha_1, \alpha_2) &= \frac{\alpha_1}{4\pi} \hat{J}_{s,0} \hat{U}_0(\alpha_1, \alpha_2) - \frac{\alpha_2}{4\pi} \hat{U}_0(\alpha_1, \alpha_2) \hat{J}_{s,0} \\ &+ \frac{\alpha_1 \ln \alpha_1}{4\pi} \hat{J}_{s,1} \hat{U}_0(\alpha_1, \alpha_2) - \frac{\alpha_2 \ln \alpha_2}{4\pi} \hat{U}_0(\alpha_1, \alpha_2) \hat{J}_{s,1}. \end{aligned} \quad (2.44)$$

In the three-flavor regime, the matrix $\hat{J}_{s,0}$ in eq. (2.30) contains an undetermined component t_s . Since the first and second term of \hat{U}_{QCD} in eq. (2.44) depend on different scales, one naively could argue that the cancellation of any dependence has to take place for each term independently of the other. However, we will show that this is not the case.

We locate the undetermined parameter in $[\hat{J}_{s,0}]_{8,7} = t_s$. The matrix product $\hat{J}_{s,0}\hat{U}_0(\alpha_1, \alpha_2)$ naturally contains a dependence on t_s in the 8th row. Actually, this dependence does cancel for all elements except for $[\hat{J}_{s,0}U_0(\alpha_1, \alpha_2)]_{8,7} \supset (\alpha_2/\alpha_1)^{1/9}t_s$. The matrix product $\hat{U}_0(\alpha_1, \alpha_2)\hat{J}_{s,0}$ in the second term of \hat{U}_{QCD} naturally obtains the parameter t_s in the 7th column, and again the product consistently cancels this dependence for all entries except for $[\hat{U}_0(\alpha_1, \alpha_2)\hat{J}_{s,0}]_{8,7} \supset (\alpha_2/\alpha_1)^{-8/9}t_s$. The full cancellations is thus only achieved by taking both terms of the first line of eq. (2.44) into account and takes the form

$$\begin{aligned} \left[\frac{\alpha_1}{4\pi} \hat{U}_{\text{QCD}}(\alpha_1, \alpha_2) \right]_{8,7} &\supset \left[\frac{\alpha_1}{4\pi} \hat{J}_{s,0} \hat{U}_0(\alpha_1, \alpha_2) - \frac{\alpha_2}{4\pi} \hat{U}_0(\alpha_1, \alpha_2) \hat{J}_{s,0} \right]_{8,7} \\ &\supset \frac{1}{4\pi} \left(\alpha_1 \left(\frac{\alpha_2}{\alpha_1} \right)^{\frac{1}{9}} - \alpha_2 \left(\frac{\alpha_2}{\alpha_1} \right)^{-\frac{8}{9}} \right) t_s \\ &= 0. \end{aligned} \quad (2.45)$$

The reason that causes the singularity to arise — eigenvalues of $\hat{\gamma}_s^{(0)T}$ differing by $2\beta_0$ in eq. (2.15) — is also responsible for the cancellation of the undetermined parameter between the high and low scales. The difference of two eigenvalues of $\hat{\gamma}_s^{(0)T}$ by $2\beta_0$ causes a difference of 1 in the exponents of (α_2/α_1) and indeed the spectrum of $\hat{\gamma}_s^{(0)T}/2\beta_0$ contains both $1/9$ and $-8/9$ as eigenvalues. Thus, this difference allows the prefactors α_1 and α_2 of the first two terms in eq. (2.44) to exactly cancel these terms between the different scales and entirely independent on the actual size of the scales.

Next, we focus on the arbitrary parameter t_e which appears in the matrix $\hat{J}_{e,0}$ in eq. (2.32) in the three flavor regime and must cancel in the \hat{U}_{QED} part of the evolution matrix. Let us denote the t_e -dependent piece of $\hat{J}_{e,0}$ with \hat{t}_e , where $[\hat{t}_e]_{7,7} = t_e$, $[\hat{t}_e]_{7,8} = 3t_e$, $[\hat{t}_e]_{8,7} = -t_e/3$, $[\hat{t}_e]_{8,8} = -t_e$, and the other components are zero. Using the matrix \hat{V} it can be written as $\hat{t}_e = \hat{V} \hat{t}'_e \hat{V}^{-1}$, where $[\hat{t}'_e]_{10,1} = -t_e$ and the other components are zero. Then, in the evolution matrix, the t_e dependence takes the following form:

$$\begin{aligned} \frac{\alpha_{\text{EM}}}{\alpha_1} \hat{U}_{\text{QED}}(\alpha_1, \alpha_2) &\supset \alpha_{\text{EM}} \left(\frac{1}{\alpha_1} \hat{J}_{e,0} \hat{U}_0(\alpha_1, \alpha_2) - \frac{1}{\alpha_2} \hat{U}_0(\alpha_1, \alpha_2) \hat{J}_{e,0} \right) \\ &\supset \alpha_{\text{EM}} \hat{V} \left(\frac{1}{\alpha_1} \hat{t}'_e \hat{U}_{0,D}(\alpha_1, \alpha_2) - \frac{1}{\alpha_2} \hat{U}_{0,D}(\alpha_1, \alpha_2) \hat{t}'_e \right) \hat{V}^{-1}, \end{aligned} \quad (2.46)$$

where $\hat{U}_{0,D}(\alpha_1, \alpha_2)$ is defined as

$$\hat{U}_0(\alpha_1, \alpha_2) = \hat{V} \text{diag} \left(\left(\frac{\alpha_2}{\alpha_1} \right)^{\frac{(\hat{\gamma}_{s,D}^{(0)T})_{1,1}}{2\beta_0}}, \left(\frac{\alpha_2}{\alpha_1} \right)^{\frac{(\hat{\gamma}_{s,D}^{(0)T})_{2,2}}{2\beta_0}}, \dots, \left(\frac{\alpha_2}{\alpha_1} \right)^{\frac{(\hat{\gamma}_{s,D}^{(0)T})_{10,10}}{2\beta_0}} \right) \hat{V}^{-1} \quad (2.47)$$

$$\equiv \hat{V} \hat{U}_{0,D}(\alpha_1, \alpha_2) \hat{V}^{-1}. \quad (2.48)$$

All components except for (10, 1) of the parenthesis in eq. (2.46) are zero trivially. The cancellation of the (10, 1) component then proceeds in the same way as in the QCD case:

$$\begin{aligned} \left[\frac{1}{\alpha_1} \hat{t}'_e \hat{U}_{0,D}(\alpha_1, \alpha_2) - \frac{1}{\alpha_2} \hat{U}_{0,D}(\alpha_1, \alpha_2) \hat{t}'_e \right]_{10,1} &= \left(\frac{1}{\alpha_1} \left(\frac{\alpha_2}{\alpha_1} \right)^{-\frac{8}{9}} - \frac{1}{\alpha_2} \left(\frac{\alpha_2}{\alpha_1} \right)^{\frac{1}{9}} \right) \cdot (-t_e) \\ &= 0. \end{aligned} \tag{2.49}$$

Therefore, the t_e dependence of \hat{U}_{QED} vanishes.

The cancellation of the parameters $t_{se1,2,\dots,14}$ in the second matrix product of eq. (2.34) is more trivial. Let us define the second matrix product as $\hat{V} \hat{t}_{se} \hat{V}^{-1}$. In the evolution matrix, the matrix \hat{t}_{se} appears only in the $\hat{U}_{\text{QCD-QED}}$ part and the cancellation can be understood in the following way:

$$\begin{aligned} \frac{\alpha_{\text{EM}}}{4\pi} \hat{U}_{\text{QCD-QED}}(\alpha_1, \alpha_2) &\supset \frac{\alpha_{\text{EM}}}{4\pi} \left(\hat{J}_{se,0} \hat{U}_0(\alpha_1, \alpha_2) - \hat{U}_0(\alpha_1, \alpha_2) \hat{J}_{se,0} \right) \\ &\supset \frac{\alpha_{\text{EM}}}{4\pi} \hat{V} \left[\hat{t}_{se}, \hat{U}_{0,D}(\alpha_1, \alpha_2) \right] \hat{V}^{-1} \\ &= 0, \end{aligned} \tag{2.50}$$

where we use the fact that $(\hat{\gamma}_{s,D}^{(0)T})_{3,3} = (\hat{\gamma}_{s,D}^{(0)T})_{4,4}$ and $(\hat{\gamma}_{s,D}^{(0)T})_{7,7} = (\hat{\gamma}_{s,D}^{(0)T})_{8,8}$ are pairwise degenerate eigenvalues for any number of active flavors.

On the contrary, the cancellation of t_s arising in $\hat{U}_{\text{QCD-QED}}$ and t_e in $\hat{U}_{\text{QED-QED}}$ is highly non-trivial. The t_s dependence, for example, resides in $\hat{J}_{s,0}$, $\hat{J}_{se,0}$ and $\hat{J}_{se,1}$ which appear in the matrix $\hat{U}_{\text{QCD-QED}}$. Logarithmic α_s terms are accompanied by $\hat{J}_{se,1}$ and by the matrix products $\hat{J}_s \hat{U}_{\text{QED}}$ and $\hat{U}_{\text{QED}} \hat{J}_s$. Although we do not give an analytic explanation for these cancellations in this paper, we have checked that taking the sum of all terms in eqs. (2.42) and (2.43) eliminates any t_s and t_e dependence of $\hat{U}_{\text{QCD-QED}}$ and $\hat{U}_{\text{QED-QED}}$.

Now we have shown that the evolution matrix in eq. (2.39) is independent of the undetermined parameters, so that we can set them to arbitrary values from the beginning. These parameters are directly related to the singular components in eqs. (2.15), (2.16) of the standard solution in the literature. Therefore, our method automatically regularizes all singularities and these parameters correspond to the choices of the finite pieces of the regulated expressions, which can therefore be viewed as scheme parameters.

We have also found that the cancellation of the parameters occurs between the high and low scales. This insight is especially important when considering new physics at a high scale. The Wilson coefficients for a given model are typically calculated at leading order only. In the evolution to the scale of 1 GeV appropriate for Kaon physics one then usually neglects the corrections to \hat{K}' in eq. (2.7) justified by the smallness of $\alpha_s(\mu_2)$ compared to $\alpha_s(\mu_1)$. In the typical applications in flavor physics, which do not involve corrections of order α_{EM} , this procedure is scheme-independent. We here show that such a treatment is inconsistent in view of the cancellation of the singularity regulating scheme parameters.

This inconsistency does not appear in the QCD and QED parts which are nonsingular at $f = 4, 5, 6$. However the combined QCD-QED part, in which singularities persist for all numbers of flavors, will yield results depending on unphysical arbitrary scheme parameters

if parts of the evolution matrix are discarded in the described way. Instead, the pieces of \hat{K}' which depend on the scheme parameters t_{se} must be consistently retained.

2.4 Validation of the logarithmic contribution

Finally, let us comment on the logarithmic contributions $\hat{J}_{s,1}$ and $\hat{J}_{e,1}$. At the $\mathcal{O}(\alpha_s)$ part, we have the following logarithmic contributions to the evolution matrix,

$$\begin{aligned} \hat{U}_f(\alpha_1, \alpha_2) &\supset \frac{\alpha_1}{4\pi} \hat{U}_{\text{QCD}}(\alpha_1, \alpha_2) \\ &\supset \frac{1}{4\pi} \left(\alpha_1 \ln \alpha_1 \hat{J}_{s,1} \hat{U}_0(\alpha_1, \alpha_2) - \alpha_2 \ln \alpha_2 \hat{U}_0(\alpha_1, \alpha_2) \hat{J}_{s,1} \right) \end{aligned} \quad (2.52)$$

$$= \frac{\alpha_1}{4\pi} \left(\frac{\alpha_2}{\alpha_1} \right)^{\frac{1}{9}} \ln \frac{\alpha_1}{\alpha_2} \hat{J}_{s,1}. \quad (2.53)$$

In the $\hat{J}_{s,1}$ matrix, the only nonzero component is $[\hat{J}_{s,1}]_{8,7} = -10/27$. Using a calculation parallel to the one in the previous subsection, we find that the only nonzero component in the matrix product $\hat{J}_{s,1} \hat{U}_0(\alpha_1, \alpha_2)$ is $[\hat{J}_{s,1} \hat{U}_0(\alpha_1, \alpha_2)]_{8,7} = (\alpha_2/\alpha_1)^{1/9} \cdot (-10/27)$, and similarly $[\hat{U}_0(\alpha_1, \alpha_2) \hat{J}_{s,1}]_{8,7} = (\alpha_2/\alpha_1)^{-8/9} \cdot (-10/27)$. Then, the (8, 7) component in the parenthesis in eq. (2.52) becomes $-(10/27)\alpha_1(\alpha_2/\alpha_1)^{1/9} \ln(\alpha_1/\alpha_2)$, and we arrive at eq. (2.53). We find that this result is consistent with eq. (40) of ref. [25], where, in order to regulate the singularity, a small regulator ϵ is introduced in the eigenvalues of $\hat{\gamma}_s^{(0)T}$.

With a similar calculation for the $\mathcal{O}(\alpha_{\text{EM}}/\alpha_s)$ part we obtain the following term,

$$\begin{aligned} \hat{U}_f(\alpha_1, \alpha_2) &\supset \frac{\alpha_{\text{EM}}}{\alpha_1} \hat{U}_{\text{QED}}(\alpha_1, \alpha_2) \\ &\supset \alpha_{\text{EM}} \left(\frac{1}{\alpha_1} \ln \alpha_1 \hat{J}_{e,1} \hat{U}_0(\alpha_1, \alpha_2) - \frac{1}{\alpha_2} \ln \alpha_2 \hat{U}_0(\alpha_1, \alpha_2) \hat{J}_{e,1} \right) \\ &= \alpha_{\text{EM}} \left(\frac{1}{\alpha_1} \ln \alpha_1 \left(\frac{\alpha_2}{\alpha_1} \right)^{-\frac{8}{9}} - \frac{1}{\alpha_2} \ln \alpha_2 \left(\frac{\alpha_2}{\alpha_1} \right)^{\frac{1}{9}} \right) \hat{J}_{e,1} \\ &= \frac{\alpha_{\text{EM}}}{\alpha_1} \left(\frac{\alpha_2}{\alpha_1} \right)^{-\frac{8}{9}} \ln \frac{\alpha_1}{\alpha_2} \hat{J}_{e,1}. \end{aligned} \quad (2.54)$$

This logarithmic contribution is also consistent with eq. (2.28) of ref. [13].

2.5 Higher orders in α_{EM} and comparison with ref. [22]

The RG evolution in the pioneering papers [5, 6, 13] discards all terms which are quadratic or higher-order in α_{EM} . Our solution in eq. (2.39) is correct to order $\alpha_{\text{EM}}^2/\alpha_s^2$, but neglects terms of order $\alpha_{\text{EM}}^2/\alpha_s$ and higher. The extra term is numerically unimportant for the SM analysis, but matters in studies of new-physics contributions generated at very high scales, where α_s is small. We come back to this point in section 4.2. The RG evolution derived in ref. [22] considers terms quadratic in α_{EM} , including terms of order $\alpha_{\text{EM}}^2/\alpha_s$ which we neglect. In particular, the μ dependence of α_{EM} affects the RG evolution at order $\alpha_{\text{EM}}^2/\alpha_s^2$ and is therefore also included in ref. [22]. While ref. [22] addresses B decays, the derived formulae equally apply to ϵ'_K and were used in ref. [14]. We argue that the inclusion of

$\alpha_{\text{EM}}^2/\alpha_s$ terms in the RGE does not improve the prediction of ϵ'_K/ϵ_K , because other terms of the same order are not included in the standard NLO solution: for instance, at this order the two-loop pure QED anomalous dimension matrix $\hat{\gamma}_e^{(1)}$ must be added to $\hat{\gamma}(g_s(\mu))$ in eq. (2.4).

Another issue are the $\Delta I = 1/2$ operators

$$Q_{11} = (\bar{s}_\alpha d_\alpha)_{V-A} (\bar{b}_\beta b_\beta)_{V-A}, \quad Q_{12} = (\bar{s}_\alpha d_\beta)_{V-A} (\bar{b}_\beta b_\alpha)_{V-A}, \quad (2.55)$$

which are generated by electroweak box diagrams, so that their Wilson coefficients are of order α_{EM} . In agreement with ref. [6] we find a small impact of these operators, contributing (-0.07×10^{-4}) to ϵ'_K/ϵ_K . Furthermore, this contribution dominantly comes from A_2 which is entered by $Q_{11,12}$ through RG mixing triggered by $\hat{\gamma}_e^{(0)}$ and is thus $\mathcal{O}(\alpha_{\text{EM}}^2/\alpha_s)$ and to be discarded. While the contribution of $Q_{11,12}$ to A_0 is formally part of the NLO solution for ϵ'_K/ϵ_K , it is numerically completely negligible (contributing -0.01×10^{-4}).

We close this section by comparing our solution of the RG equations in eqs. (2.17)–(2.29) to the one in ref. [22]. Actually, the latter also regulates all the singularities by logarithmic terms, and uses the diagonalisation of $\hat{\gamma}_s^{(0)}$ as described before eq. (2.15). The matrices \hat{J}_{\dots} transform into $\hat{J}_{\dots,D} \equiv \hat{V}^{-1} \hat{J}_{\dots} \hat{V}$ when passing to the diagonal basis. Therefore eqs. (2.21)–(2.29) also hold with the replacements $\hat{\gamma}_s^{(0)} \rightarrow \hat{\gamma}_{s,D}^{(0)}$ and $\hat{J}_{\dots} \rightarrow \hat{J}_{\dots,D}$. In this form one can most easily compare our result with eq. (47) of ref. [22]. The \hat{U}_0 , \hat{U}_{QCD} , \hat{U}_{QED} , $\hat{U}_{\text{QCD-QED}}$, and $\hat{U}_{\text{QED-QED}}$ correspond to $\mathcal{O}(\omega^0 \lambda^0)$, $\mathcal{O}(\omega)$, $\mathcal{O}(\lambda)$, $\mathcal{O}(\omega \lambda)$, and $\mathcal{O}(\lambda^2)$ terms in ref. [22], respectively. We have checked that our formulae of the RG evolution matrices are numerically equivalent to those in ref. [22]. We find that our solution is easier to implement and leads to a faster numerical evaluation.

3 ϵ'_K/ϵ_K in the Standard Model at next-to-leading order

In this section, we evaluate ϵ'_K/ϵ_K in the Standard Model at next-to-leading order, using the evolution matrix derived in the previous section.

We calculate the Wilson coefficients v_i and z_i in eqs. (2.1) and (2.2) with the methodology of ref. [13]. Throughout this paper, the $\overline{\text{MS}}$ -NDR regularization scheme is used. For the next-to-leading order RG evolution of the Wilson coefficients, we use the singularity-free evolution matrix in eq. (2.39) and systematically discard higher-order contributions. Table 1 shows our result of the Wilson coefficients at $\mu = 1.3 \text{ GeV}$, where $y_i \equiv v_i - z_i$. We decompose y_i into the LO contribution $\mathcal{O}(1)$ and the four $\mathcal{O}(\alpha_{\text{EM}}/\alpha_s, \alpha_s, \alpha_{\text{EM}}, \alpha_{\text{EM}}^2/\alpha_s^2)$ NLO terms, where $\mathcal{O}(1)$ refers to tree-level W -boson exchange combined with the one-gluon anomalous dimension matrix $\hat{\gamma}_s^{(0)}$ in the RG evolution. Here we take $\alpha_s(M_Z) = 0.1185$, $\alpha_{\text{EM}}(M_W) = 1/128$, $m_t = 163.3 \text{ GeV}$, $m_b = 4.18 \text{ GeV}$, and $\mu_c = 1.4 \text{ GeV}$, which is the threshold scale between three and four flavor effective theories in eqs. (2.1) and (2.2). Note that we include $\ln(m_c^2/\mu_c^2)$ contributions in the charm quark threshold correction $z_i(\mu_c)$ in eq. (2.2), where we use $m_c = 1.275 \text{ GeV}$ [29]. To calculate $\alpha_s(\mu)$ we use `RunDec:v1.0` with two-loop accuracy [30].

Next we take the hadronic matrix elements from a recent lattice QCD calculation [17–20], using the real parts (CP -conserving parts) of the isospin amplitudes $A_{I=0,2} =$

i	$z_i(\mu)$	$y_i(\mu)$	$\mathcal{O}(1)$	$\mathcal{O}(\alpha_{\text{EM}}/\alpha_s)$	$\mathcal{O}(\alpha_s)$	$\mathcal{O}(\alpha_{\text{EM}})$	$\mathcal{O}(\alpha_{\text{EM}}^2/\alpha_s^2)$
1	-0.3903	0	0	0	0	0	0
2	1.200	0	0	0	0	0	0
3	0.0044	0.0275	0.0254	0.0001	0.0007	0.0012	0
4	-0.0131	-0.0566	-0.0485	-0.0002	-0.0069	-0.0009	0
5	0.0039	0.0068	0.0124	0.0001	-0.0059	0.0001	0
6	-0.0128	-0.0847	-0.0736	-0.0003	-0.0099	-0.0008	0
$7/\alpha_{\text{EM}}$	0.0040	-0.0321	0	-0.1116	0	0.0760	0.0035
$8/\alpha_{\text{EM}}$	0.0019	0.1148	0	-0.0227	0	0.1366	0.0009
$9/\alpha_{\text{EM}}$	0.0051	-1.3815	0	-0.1267	0	-1.2581	0.0034
$10/\alpha_{\text{EM}}$	-0.0013	0.4883	0	0.0217	0	0.4672	-0.0006

Table 1. Wilson coefficients at $\mu = 1.3 \text{ GeV}$, where the 7–10th components are divided by $\alpha_{\text{EM}}(M_W)$. y_i is decomposed into the LO contribution and the individual NLO corrections.

$\langle (\pi\pi)_{I=0,2} | \mathcal{H}_{\text{eff}}^{|\Delta S|=1} | K^0 \rangle$ as additional constraints [13]. These amplitudes have been measured very precisely [19],

$$\text{Re } A_0 = (3.3201 \pm 0.0018) \times 10^{-7} \text{ GeV}, \tag{3.1}$$

$$\text{Re } A_2 = (1.4787 \pm 0.0031) \times 10^{-8} \text{ GeV}. \tag{3.2}$$

Since the real parts are dominated by Standard-Model tree-level coefficients z_2 (see table 1), they can be used to fix one of the hadronic matrix elements $\langle (\pi\pi)_I | Q_i(\mu) | K^0 \rangle \equiv \langle Q_i(\mu) \rangle_I$. $\langle Q_2 \rangle_0$ dominates the real part of A_0 , but contributes to the imaginary part only through the operator Fierz relations¹

$$Q_4 = -Q_1 + Q_2 + Q_3, \quad Q_{10} = Q_2 + \frac{1}{2}(Q_1 - Q_3). \tag{3.3}$$

$\langle Q_1 \rangle_0$ is the second largest contribution and the remaining matrix elements are almost negligible. The situation is more handy in the case of A_2 , where the real part is parameterized entirely by $\langle Q_2 \rangle_2$ due to the fact that $\langle Q_1 \rangle_2 = \langle Q_2 \rangle_2$ in pure QCD [6, 13]. In our analysis we derive values of $\langle Q_2 \rangle_0$ and $\langle Q_2 \rangle_2$ at the scale μ from the experimental measurements of $\text{Re } A_0$ and $\text{Re } A_2$, respectively.²

¹The Fierz relation for Q_4 is modified by $\mathcal{O}(\alpha_s/4\pi)$ corrections [13], but these contributions are numerically small [14].

²On the other hand, once one introduces the ratio

$$q = \frac{z_+(\mu) (\langle Q_2 \rangle_0 + \langle Q_1 \rangle_0)}{z_-(\mu) (\langle Q_2 \rangle_0 - \langle Q_1 \rangle_0)} \quad \text{with} \quad z_{\pm}(\mu) = z_2(\mu) \pm z_1(\mu), \tag{3.4}$$

one can calculate $\text{Im } A_I / \text{Re } A_I$ without using the fit of $\langle Q_2 \rangle_I$ to the data. Ref. [14] uses this strategy with the parameter range $0 \leq q \leq 0.1$. Basically, the difference with our method (corresponding to the q -dependent terms in ref. [14]) only affects numerically subleading contributions (the $i = 3, 4, 9, 10$ components of $\text{Im } A_0 / \text{Re } A_0$). In either method the hadronic uncertainties are reduced compared to the choice to take all matrix elements from lattice.

The decay amplitude of $K \rightarrow (\pi\pi)_{I=0}$ has been computed using a 2 + 1 flavor lattice QCD simulation at the renormalization scale $\mu = 1.531 \text{ GeV}$ [20]. In order to combine these matrix elements with the Wilson coefficients evaluated in the three-flavor regime — that is, at a scale below the charm quark mass — we need to evolve the hadronic matrix elements down to a scale below μ_c . The isospin amplitude is given as

$$\begin{aligned} A_I &= \frac{G_F}{\sqrt{2}} \lambda_u \langle \vec{Q}(\mu_1)^T \rangle_I \vec{C}(\mu_1) \\ &= \frac{G_F}{\sqrt{2}} \lambda_u \langle \vec{Q}(\mu_1)^T \rangle_I \hat{U}_3(\mu_1, \mu_2) \vec{C}(\mu_2) \\ &= \frac{G_F}{\sqrt{2}} \lambda_u \langle \vec{Q}(\mu_2)^T \rangle_I \vec{C}(\mu_2), \end{aligned} \tag{3.5}$$

where $\mu_1 < \mu_2$ and $C_i(\mu) \equiv z_i(\mu) + \tau y_i(\mu)$. In the final line, we use the fact that the physical amplitude A_I is independent of the renormalization scale, so that

$$\langle \vec{Q}(\mu_1)^T \rangle_I = \langle \vec{Q}(\mu_2)^T \rangle_I \left(\hat{U}_3(\mu_1, \mu_2) \right)^{-1}. \tag{3.6}$$

In practice, we first evaluate the hadronic matrix elements for the $I = 0$ states at $\mu = 1.3 \text{ GeV}$ from the lattice results [20] using a three flavor evolution matrix, cf. eq. (3.6). Here we use $\alpha_s^{(3)}(1.531 \text{ GeV}) = 0.353388$ as in the lattice calculation of ref. [20]. Then we determine $\langle Q_2(\mu) \rangle_0$ (and $\langle Q_{4,10}(\mu) \rangle_0$ through eq. (3.3)) from the experimental value of $\text{Re } A_0$ using the Wilson coefficients shown in table 1. We have taken the CKM parameters from CKMfitter [31]. The results are shown in table 2a.

The decay amplitude of $K \rightarrow (\pi\pi)_{I=2}$ has also been computed using a 2+1 flavor lattice QCD simulations, albeit at the scale $\mu = 3.0 \text{ GeV}$ [17–19]. According to ref. [18], one can extract the lattice results in an operator basis renormalized by the $\overline{\text{MS}}$ -NDR regularization scheme. From ref. [19], which is the latest lattice QCD calculation for $I = 2$, we obtain

$$\mathcal{M}_{(27,1)}^{\overline{\text{MS}}\text{-NDR}}(3 \text{ GeV}) = 3\sqrt{3} \langle Q_1(3 \text{ GeV}) \rangle_2 = 0.0502 \pm 0.0031 \text{ (GeV)}^3, \tag{3.7}$$

$$\mathcal{M}_{(8,8)}^{\overline{\text{MS}}\text{-NDR}}(3 \text{ GeV}) = 2\sqrt{3} \langle Q_7(3 \text{ GeV}) \rangle_2 = 0.993 \pm 0.038 \text{ (GeV)}^3, \tag{3.8}$$

$$\mathcal{M}_{(8,8)_{\text{mix}}}^{\overline{\text{MS}}\text{-NDR}}(3 \text{ GeV}) = 2\sqrt{3} \langle Q_8(3 \text{ GeV}) \rangle_2 = 4.547 \pm 0.275 \text{ (GeV)}^3, \tag{3.9}$$

where the results of the (\not{q}, \not{q}) intermediate scheme are taken as central value, while the results of the (γ^μ, γ^μ) scheme are taken as uncertainty. Using the three flavor evolution matrix in eq. (3.6), we obtain the hadronic matrix elements at $\mu = 1.3 \text{ GeV}$ for the $I = 2$ states. Here, we use the lattice input α_s value: $\alpha_s^{(3)}(3 \text{ GeV}) = 0.24544$ [18]. Then, from the experimental value of $\text{Re } A_2$ we determine $\langle Q_2(\mu) \rangle_2$ (and $\langle Q_{1,9,10}(\mu) \rangle_2$ through eq. (3.3), $\langle Q_1(\mu) \rangle_2 = \langle Q_2(\mu) \rangle_2$ and $Q_9 = \frac{1}{2}(3Q_1 - Q_3)$ which is a Fierz relation). The results are shown in table 2b. Note that through the evolution matrices \hat{U}_{QED} and $\hat{U}_{\text{QCD-QED}}$ this procedure generates small nonzero values of $\langle Q_{3-6}(\mu) \rangle_2$, which are regarded as non-electroweak penguin contributions to $\text{Im } A_2$. Since the lattice simulations have not calculated them at 3.0 GeV, one should not use them at the lower hadronic scale μ . On the other hand, they have been calculated with chiral perturbation theory [15, 16] and are included in the

i	$\langle Q_i(\mu) \rangle_0^{\overline{\text{MS}}\text{-NDR}} (\text{GeV})^3$
1	-0.144 ± 0.046
2	0.105 ± 0.015
3	-0.040 ± 0.068
4	0.210 ± 0.069
5	-0.179 ± 0.068
6	-0.338 ± 0.121
7	0.154 ± 0.065
8	1.540 ± 0.372
9	-0.197 ± 0.070
10	0.053 ± 0.038

i	$\langle Q_i(\mu) \rangle_2^{\overline{\text{MS}}\text{-NDR}} (\text{GeV})^3$
1	0.01006 ± 0.00002
2	0.01006 ± 0.00002
3	—
4	—
5	—
6	—
7	0.127 ± 0.012
8	0.852 ± 0.052
9	0.01509 ± 0.00003
10	0.01509 ± 0.00003

(a)
(b)

$B_1^{(1/2)}(\mu)$	35.5 ± 11.2
$B_2^{(1/2)}(\mu)$	5.17 ± 0.71
$B_3^{(1/2)}(\mu)$	-3.27 ± 5.60
$B_5^{(1/2)}(\mu)$	0.88 ± 0.33
$B_6^{(1/2)}(\mu)$	0.56 ± 0.20
$B_7^{(1/2)}(\mu)$	0.24 ± 0.10
$B_8^{(1/2)}(\mu)$	0.98 ± 0.24
$B_1^{(3/2)}(\mu)$	0.437 ± 0.001
$B_7^{(3/2)}(\mu)$	0.37 ± 0.03
$B_8^{(3/2)}(\mu)$	0.77 ± 0.05

(c)

Table 2. The hadronic matrix elements (a), (b) and B parameters (c) extracted from the lattice calculations for $I = 0$ [20] and $I = 2$ [19]. The experimental values of the real parts of the amplitudes have been used [19]. The large errors result from the quoted lattice errors on the hadronic matrix elements. The experimental errors are small in comparison. We take $\mu = 1.3$ GeV.

isospin-violating corrections $\hat{\Omega}_{\text{eff}}$ of eq. (1.1).³ Therefore, we have decided to omit these contributions at the hadronic scale μ .

To compare with the literature, we also extract B parameters from the hadronic matrix elements in table 2c. These B parameters are defined as in ref. [14]:

$$\langle Q_6(\mu) \rangle_0 = -4\sqrt{\frac{3}{2}} \left(\frac{m_K^2}{m_s(\mu) + m_d(\mu)} \right)^2 (F_K - F_\pi) B_6^{(1/2)}(\mu), \quad (3.10)$$

$$\langle Q_8(\mu) \rangle_2 = \sqrt{3} \left(\frac{m_K^2}{m_s(\mu) + m_d(\mu)} \right)^2 F_\pi B_8^{(3/2)}(\mu). \quad (3.11)$$

All other B parameters are defined in ref. [13]. For running quark masses, we use the lattice results $m_s(2\text{ GeV}) = 93.8(2.4)\text{ MeV}$ and $m_d(2\text{ GeV}) = 4.68(16)\text{ MeV}$ with the three-flavor RG evolution [32]. Since the uncertainty from the strange quark mass is already included in the lattice results of $\langle Q_i \rangle_I$ as one of the systematic errors, we do not include it in the estimation of uncertainties of the B parameters. The B parameters are consistent with ref. [14], and we also confirmed the almost μ -independent behavior of $B_6^{(1/2)}(\mu)$ and $B_8^{(3/2)}(\mu)$ [13]. Note that in the following analysis we will directly use the hadronic matrix elements $\langle Q_i \rangle_I$ rather than the B parameters.

Finally we combine the short-distance and long-distance contributions. The master equation of ϵ'_K/ϵ_K is given in eq. (1.1). Since the isospin-violating correction by the electroweak penguins to $\text{Im } A_0$ are already subtracted from $\hat{\Omega}_{\text{eff}}$ as $\langle Q_{7-10} \rangle_0$, one should evaluate the last term in eq. (1.1) as

$$(1 - \hat{\Omega}_{\text{eff}}) \text{Im } A_0 = (1 - \hat{\Omega}_{\text{eff}}) (\text{Im } A_0)^{\text{others}} + \frac{1}{a} (\text{Im } A_0)^{\text{EWP}}, \quad a = 1.017, \quad (3.12)$$

with the two terms representing the contributions from $\langle Q_{3-6} \rangle_0$ and $\langle Q_{7-10} \rangle_0$, respectively [14]. In addition, the experimental values of $\text{Re } A_0$ in eq. (3.1) and $|\epsilon_K| = 2.228 \times 10^{-3}$ [29] are used. Our result for ϵ'_K/ϵ_K in the Standard Model at the next-to-leading order is

$$\left(\frac{\epsilon'_K}{\epsilon_K} \right)_{\text{SM-NLO}} = (1.06 \pm 4.66_{\text{Lattice}} \pm 1.91_{\text{NNLO}} \pm 0.59_{\text{IV}} \pm 0.23_{m_t}) \times 10^{-4}. \quad (3.13)$$

The first error originates from the lattice-QCD simulations [19, 20] and is dominated by the uncertainty stemming from $\langle Q_6 \rangle_0$ (which is $\pm 4.52 \times 10^{-4}$) (see figure 2c). The uncertainties from $\langle Q_3 \rangle_0$ through eq. (3.3) and from $\langle Q_8 \rangle_2$ are subleading ($\pm 0.77 \times 10^{-4}$ and $\pm 0.56 \times 10^{-4}$, respectively).

The second uncertainty comes from perturbative higher-order corrections, which we estimate in two ways. Firstly, we estimate uncertainties from higher-order corrections to the Wilson coefficients by calculating the RG evolution of the Wilson coefficients with a different method. Instead of using the analytic evolution matrices formulated in section 2, we solve the corresponding set of differential equations numerically.

$$\frac{d\vec{v}(\mu)}{d \ln \mu} = \hat{\gamma}^T(g_s(\mu))\vec{v}(\mu), \quad \frac{d\vec{z}(\mu)}{d \ln \mu} = \hat{\gamma}^T(g_s(\mu))\vec{z}(\mu). \quad (3.14)$$

³The non-electroweak penguin contributions are calculated at $\mu = 1.0 \pm 0.3\text{ GeV}$ [15, 16].

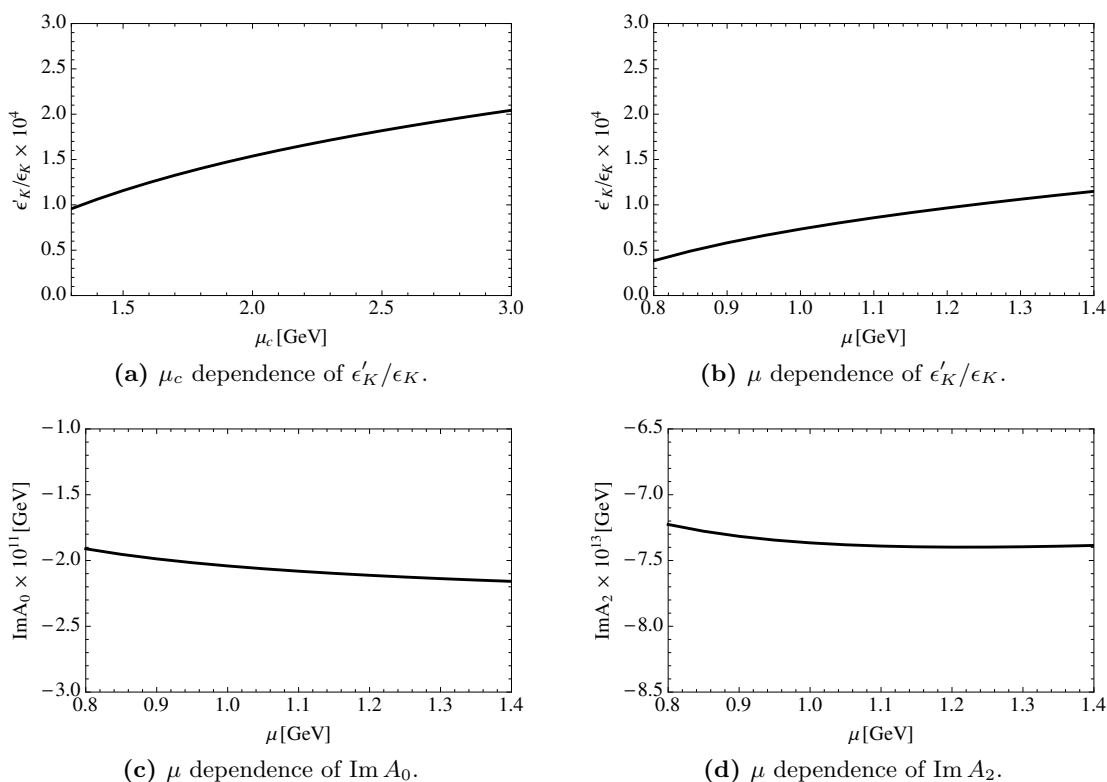


Figure 1. (a) The μ_c dependence of ϵ'_K/ϵ_K in the range $1.3 < \mu_c < 3.0$ GeV with $\mu = 1.3$ GeV. The μ dependence of ϵ'_K/ϵ_K (b), $\text{Im } A_0$ (c) and $\text{Im } A_2$ (d) in the range $0.8 < \mu < 1.4$ GeV with $\mu_c = 1.4$ GeV.

Since this RG evolution contains higher-order (namely $\mathcal{O}(\alpha_s^2, \alpha_s \alpha_{\text{EM}})$) corrections, the result is interpreted as a conservative estimate of the uncertainty in the short-distance contributions. As a result, we find that the Wilson coefficients are shifted by about 10 percent compared with table 1, and we obtain $\epsilon'_K/\epsilon_K = -0.32 \times 10^{-4}$. Hence, we estimate that the uncertainty from higher-order corrections is $\pm 1.38 \times 10^{-4}$. Secondly, we have investigated the μ_c and μ dependences of ϵ'_K/ϵ_K . In figure 1a, we show the μ_c dependence of ϵ'_K/ϵ_K in the range $1.3 < \mu_c < 3.0$ GeV with fixed $\mu = 1.3$ GeV. In figure 1b, we vary μ with μ_c fixed at 1.4 GeV. We find that the μ dependence is small, $\pm 0.77 \times 10^{-4}$, while the μ_c dependence is slightly larger, $\pm 1.09 \times 10^{-4}$. The scale μ enters the prediction in three ways: first, the decomposition of the isospin-violating corrections in eq. (3.12) is imposed at this scale. Second, the omitted non-electroweak penguin contributions to $\text{Im } A_2$ depend on μ , and third, the experimental values of $\text{Re } A_0$ and $\text{Re } A_2$ to fix $\langle Q_2(\mu) \rangle_2$ and $\langle Q_2(\mu) \rangle_0$ are imposed at the hadronic scale μ . In this process, we double-count the uncertainty from the isospin-violating contributions, however, we find that these uncertainties are very small compared with the uncertainties stemming from lattice and thus we have not investigated them any further. We show the μ dependences of $\text{Im } A_0$ (and *not* the μ dependence of $(1 - \hat{\Omega}_{\text{eff}}) \text{Im } A_0$) and $\text{Im } A_2$ in figures 1c and 1d, respectively. We add the three uncertainties in quadrature. Strictly speaking, this double-counts some pieces of the unknown higher-order corrections.

The third uncertainty in eq. (3.13) stems from isospin-violating corrections [15, 16], such as strong isospin violation ($m_u \neq m_d$), non-electroweak penguin transitions in the $I = 2$ state and $\Delta I = 5/2$ corrections [33, 34]. The uncertainty is dominated by the non-electroweak penguin contributions to $\text{Im } A_2$, however, the uncertainty in ϵ'_K/ϵ_K is small.

The last uncertainty in eq. (3.13) comes from the running mass of the top quark $m_t(m_t) = 163.3 \pm 2.7 \text{ GeV}$ [35]. Since the other uncertainties we have not elaborated here are negligibly small according to ref. [14], we have omitted them in our error estimate. Therefore, our final result is

$$\left(\frac{\epsilon'_K}{\epsilon_K}\right)_{\text{SM-NLO}} = (1.06 \pm 5.07) \times 10^{-4}, \quad (3.15)$$

which is consistent with refs. [14] and [20]. On the other hand, it is well-known that the experimental value is much larger [36–41]. The current world average is [29],

$$\text{Re}\left(\frac{\epsilon'_K}{\epsilon_K}\right)_{\text{exp}} = (16.6 \pm 2.3) \times 10^{-4}. \quad (3.16)$$

We observe that our prediction of ϵ'_K/ϵ_K in the Standard Model is 2.8σ below the experimental value. This small Standard Model prediction and thus the large tension is supported by the large- N_c “dual QCD” approach [42–47], which is an entirely different approach to low energy QCD than lattice gauge theory. There has been a dispute concerning the role of final-state interactions (FSI) for the size of $\langle Q_6 \rangle_0$, with the chiral perturbation community favouring an enhancement of $\langle Q_6 \rangle_0$ by FSI [48] and an opposing view of the large- N_c community [47]. Modern lattice calculations do include FSI [49] and will speak the final word on FSI. Since the main uncertainty of the SM prediction for ϵ'_K/ϵ_K comes from statistical and systematical errors in the lattice calculation of the hadronic matrix elements for A_0 , the expected progress in this field will sharpen the Standard Model prediction in the near future [20].

We note that in absence of a lattice result for the hadronic matrix element and the smallness of the corresponding Wilson coefficient, we omit the contribution from the chromomagnetic penguin operators $Q_{8g} = m_s g_s / (16\pi^2) \bar{s} T^a \sigma_{\mu\nu} (1 - \gamma_5) d G^{\mu\nu a}$ (and the opposite-chirality analogue \tilde{Q}_{8g}). According to ref. [14], chromomagnetic penguins contribute $|0.2 - 0.7| \times 10^{-4}$,⁴ to ϵ'_K/ϵ_K , which is rather small compared with the QCD-penguin and QED-penguin contributions (see figure 2c). Even if we add this contribution as $+0.7 \times 10^{-4}$ to the central value (to the higher-order uncertainty) of ϵ'_K/ϵ_K , the discrepancy still persists at $2.7(2.8)\sigma$.

In figure 2 we show the composition of $\text{Im } A_0$, $\text{Im } A_2$ and ϵ'_K/ϵ_K with respect to the operator basis. We observe that the positive dominant contribution to ϵ'_K/ϵ_K comes from Q_6 while Q_9 is subdominant. The dominant negative contribution comes from Q_8 while Q_4 is subdominant. Remarkably, their sum almost cancels at next-to-leading order. This leads to an extremely small central value of the Standard Model prediction for ϵ'_K/ϵ_K .

⁴The sign depends on the sign of the hadronic matrix element. The preliminary lattice calculation of $\langle \pi | Q_{8g} | K \rangle$ [50] and calculations in the chiral quark model [51–53] imply that a contribution to ϵ'_K/ϵ_K is positive at the leading order. However, next-to-leading order contributions to $\langle (\pi\pi)_{I=0} | Q_{8g} | K^0 \rangle$ are expected to mess up the leading order estimate because of a parametric enhancement $\propto 1/N_c \cdot m_K^2/m_\pi^2$ [54, 55].

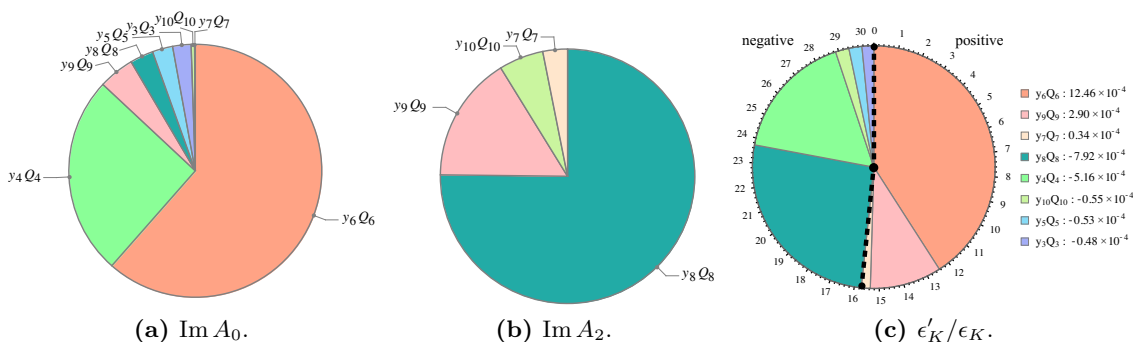


Figure 2. Composition of $\text{Im } A_0$, $\text{Im } A_2$ and ϵ'_K/ϵ_K with respect to the operator basis. We take $\mu = 1.3 \text{ GeV}$. In subfigure 2c, the right (left) side of the dashed line represents positive (negative) contributions.

Although the results of the Wilson coefficients by themselves are slightly different when compared to the result of ref. [14], the products with the hadronic matrix elements are well consistent.⁵ The main difference between this reference and our analysis is in the subleading contributions. In ref. [14], the hadronic matrix elements $\langle Q_3(\mu) \rangle_0$, $\langle Q_5(\mu) \rangle_0$ and $\langle Q_7(\mu) \rangle_0$ are set to be 0 as central values, while we have evaluated them from the lattice data. The numerical difference in ϵ'_K/ϵ_K is $\sim -1 \times 10^{-4}$. We also find that the contribution of $\mathcal{O}(\alpha_{\text{EM}}^2/\alpha_s^2)$ terms, which has not been considered in the literature so far, only contributes to ϵ'_K/ϵ_K as little as -0.10×10^{-4} . This term, however, can be relevant in new-physics models with TeV-scale isospin violation.

4 Beyond the Standard Model

4.1 Preliminaries

Upon integrating out heavy degrees of freedom in models of new physics, new contributions to Wilson coefficients of the Standard Model operators Q_i (and their opposite-chirality analogues \tilde{Q}_i) arise.

As we have shown in the previous section, the Standard Model prediction of ϵ'_K/ϵ_K is significantly below the experimental data. Although the discrepancy is only 2.8σ at present, its confirmation with higher significance by future lattice results may establish a footprint of new physics. Indeed, several new physics models can alleviate the ϵ'_K/ϵ_K tension, like generic flavor-violating Z and Z' models [56–58], 331 models [59–61], the Littlest Higgs model with T -parity [62], flavor-violating additional pseudo-scalar models [63], and the Minimal Supersymmetric Standard Model [64, 65].

Since ϵ'_K/ϵ_K is linear in the Wilson coefficients, the SM and new-physics contributions are simply additive:

$$\frac{\epsilon'_K}{\epsilon_K} = \left(\frac{\epsilon'_K}{\epsilon_K} \right)_{\text{SM}} + \left(\frac{\epsilon'_K}{\epsilon_K} \right)_{\text{NP}}. \quad (4.1)$$

⁵Indeed, the values of $y_6 \langle Q_6 \rangle_0$ and $y_8 \langle Q_8 \rangle_2$ are in good agreement with ref. [14].

Using the following effective Hamiltonian for the new physics contributions,

$$\mathcal{H}_{\text{eff, NP}}^{|\Delta S|=1} = \frac{G_F}{\sqrt{2}} \sum_{i=1}^{10} \left(Q_i(\mu) s_i(\mu) + \tilde{Q}_i(\mu) \tilde{s}_i(\mu) \right) + \text{H.c.}, \quad (4.2)$$

where the opposite-chirality operators \tilde{Q}_i are found from Q_i by interchanging $V - A \leftrightarrow V + A$, the new physics contribution is given by

$$\begin{aligned} \left(\frac{\epsilon'_K}{\epsilon_K} \right)_{\text{NP}} &= \frac{G_F \omega_+}{2 |\epsilon_K^{\text{exp}}| \text{Re } A_0^{\text{exp}}} \\ &\times \left[\frac{1}{\omega_+} \langle \vec{Q}(\mu)^T \rangle_2 \text{Im} \left[\vec{s}(\mu) - \vec{\tilde{s}}(\mu) \right] - \langle \vec{Q}(\mu)^T \rangle_0 (1 - \hat{\Omega}_{\text{eff}}) \text{Im} \left[\vec{s}(\mu) - \vec{\tilde{s}}(\mu) \right] \right] \\ &= \frac{G_F \omega_+}{2 |\epsilon_K^{\text{exp}}| \text{Re } A_0^{\text{exp}}} \left[\frac{1}{\omega_+} \langle \vec{Q}(\mu)^T \rangle_2 - \langle \vec{Q}(\mu)^T \rangle_0 (1 - \hat{\Omega}_{\text{eff}}) \right] \text{Im} \left[\vec{s}(\mu) - \vec{\tilde{s}}(\mu) \right], \\ &= \frac{G_F \omega_+}{2 |\epsilon_K^{\text{exp}}| \text{Re } A_0^{\text{exp}}} \langle \vec{Q}_{\epsilon'_K}(\mu)^T \rangle \text{Im} \left[\vec{s}(\mu) - \vec{\tilde{s}}(\mu) \right] \\ &= \frac{G_F \omega_+}{2 |\epsilon_K^{\text{exp}}| \text{Re } A_0^{\text{exp}}} \langle \vec{Q}_{\epsilon'_K}(\mu)^T \rangle \hat{U}(\mu, \mu_{\text{NP}}) \text{Im} \left[\vec{s}(\mu_{\text{NP}}) - \vec{\tilde{s}}(\mu_{\text{NP}}) \right], \end{aligned} \quad (4.3)$$

where the isospin-violating correction in eq. (3.12) is

$$\left(1 - \hat{\Omega}_{\text{eff}} \right)_{ij} = \begin{cases} 0.852 & (i = j = 1-6) \\ 0.983 & (i = j = 7-10) \\ 0 & (i \neq j), \end{cases} \quad (4.4)$$

and we employed $\langle \tilde{Q}_i(\mu) \rangle_I = -\langle Q_i(\mu) \rangle_I$ and defined $\langle \vec{Q}_{\epsilon'_K} \rangle$ as

$$\langle \vec{Q}_{\epsilon'_K}(\mu)^T \rangle \equiv \frac{1}{\omega_+} \langle \vec{Q}(\mu)^T \rangle_2 - \langle \vec{Q}(\mu)^T \rangle_0 (1 - \hat{\Omega}_{\text{eff}}). \quad (4.5)$$

The evolution matrix in eq. (4.3) is given by

$$\hat{U}(\mu, \mu_{\text{NP}}) \equiv \hat{U}_3(\mu, \mu_c) \hat{M}_c(\mu_c) \hat{U}_4(\mu_c, m_b) \hat{M}_b(m_b) \hat{U}_5(m_b, m_t) \hat{M}_t(m_t) \hat{U}_6(m_t, \mu_{\text{NP}}), \quad (4.6)$$

Since the matching matrices depend only on the difference of the number of active up- and down-type quark flavors, we take $\hat{M}_t(m) = \hat{M}_c(m)$. Note that the RG evolution of the opposite-chirality operators is the same as for the Standard Model operators and that these two sets of operators do not mix with each other. We also note that the chromomagnetic operators are omitted in our analysis.

In this section, we give a useful formula for the new physics contributions to ϵ'_K/ϵ_K considering the analytic solutions of the next-to-leading order evolutions matrices and the hadronic matrix elements we derived. We note that we omit the weak boson exchanges in the RG evolutions from μ_{NP} to M_W , where μ_{NP} represents the matching scale between the new physics and the effective Hamiltonian in eq. (4.2). Like the photon exchanges one should treat weak boson exchanges as next-to-leading contributions. Note that large

isospin violation in new-physics models enters ϵ'_K/ϵ_K through the initial conditions of the Wilson coefficients and not through the RG evolution.

We also should comment on the running of α_{EM} . Above M_W scale, we use $e(\mu_{\text{NP}}) = g(\mu_{\text{NP}})g'(\mu_{\text{NP}})/\sqrt{g^2(\mu_{\text{NP}}) + g'^2(\mu_{\text{NP}})}$, and $\beta_0^e = \beta_0^{g'}/\cos\theta_W^2(M_Z)$, where $\beta_0^{g'} = -53/9$ ($\mu < m_t$) or $-41/6$ ($\mu > m_t$). Strictly speaking, we have to consider the running of θ_W for consistency. However, we have checked that the numerical effect for an $\mathcal{O}(10 \text{ TeV})$ scale of new physics is small. Therefore we use a fixed value: $\sin^2\theta_W = 0.231$.

4.2 Counting of orders

In a full next-to-leading order estimation, we have to consider the leading order term $\mathcal{O}(1)$ arising from the one-loop QCD RG evolution as well as the terms defined as next-to-leading order, which are: the one-loop QED correction $\mathcal{O}(\alpha_{\text{EM}}/\alpha_s)$, the QCD two-loop correction $\mathcal{O}(\alpha_s)$, and the two-loop term including a photon and a gluon at $\mathcal{O}(\alpha_{\text{EM}})$. The next-to-leading order RG evolution matrix has an additional $\mathcal{O}(\alpha_{\text{EM}}^2/\alpha_s^2)$ correction, which appears only at this order. Hereafter, we will always refer to these orders when labelling perturbative quantities of the Wilson coefficients and the evolution matrices as \vec{s}_0 , \vec{s}_e , \vec{s}_s , \vec{s}_{se} , \vec{s}_{ee} and \hat{U}_0 , \hat{U}_e , \hat{U}_s , \hat{U}_{se} , \hat{U}_{ee} , respectively.

When we multiply two quantities which are given by a perturbation series, we have to carefully keep track of and consistently discard higher orders of the perturbative series. This is a subtle and cumbersome feature which complicates mathematical expressions. In this context, equations of the RG evolution should be more of a symbolic character which are exact in the limit of expanding the corresponding quantities to all orders. Since we necessarily truncate the perturbation expansion of the Wilson coefficients as well as the evolution matrices at some point, a product of them at next-to-leading order is represented as follows:

$$\begin{aligned}
 & \langle \vec{Q}_{\epsilon'_K}(\mu)^T \rangle \left(\vec{s}(\mu) - \vec{s}(\mu) \right) \\
 &= \langle \vec{Q}_{\epsilon'_K}(\mu)^T \rangle \hat{U}(\mu, \mu_{\text{NP}}) \left(\vec{s}(\mu_{\text{NP}}) - \vec{s}(\mu_{\text{NP}}) \right) \\
 &\stackrel{\text{(NLO)}}{=} \langle \vec{Q}_{\epsilon'_K}(\mu)^T \rangle (\hat{U}_0 + \hat{U}_e + \hat{U}_s + \hat{U}_{se} + \hat{U}_{ee}) (\vec{s}_0 + \vec{s}_e + \vec{s}_s + \vec{s}_{se} + \vec{s}_{ee}) \\
 &= \langle \vec{Q}_{\epsilon'_K}(\mu)^T \rangle \left(\underbrace{\hat{U}_0 \vec{s}_0}_{=:\vec{s}_0(\mu)} + \underbrace{\hat{U}_0 \vec{s}_e + \hat{U}_e \vec{s}_0}_{=:\vec{s}_e(\mu)} + \underbrace{\hat{U}_0 \vec{s}_s + \hat{U}_s \vec{s}_0}_{=:\vec{s}_s(\mu)} \right. \\
 &\quad \left. + \underbrace{\hat{U}_0 \vec{s}_{se} + \hat{U}_e \vec{s}_s + \hat{U}_s \vec{s}_e + \hat{U}_{se} \vec{s}_0}_{=:\vec{s}_{se}(\mu)} + \underbrace{\hat{U}_e \vec{s}_e + \hat{U}_{ee} \vec{s}_0 + \hat{U}_0 \vec{s}_{ee}}_{=:\vec{s}_{ee}(\mu)} \right) + \mathcal{O}\left(\frac{\alpha_{\text{EM}}^2}{\alpha_s}, \alpha_s^2, \alpha_s \alpha_{\text{EM}}, \alpha_{\text{EM}}^2\right) \\
 &= \langle \vec{Q}_{\epsilon'_K}(\mu)^T \rangle \left(\underbrace{\vec{s}_0(\mu) + \vec{s}_e(\mu) + \vec{s}_s(\mu) + \vec{s}_{se}(\mu) + \vec{s}_{ee}(\mu)}_{=:\vec{s}_{\text{NLO}}(\mu)} \right) + \mathcal{O}\left(\frac{\alpha_{\text{EM}}^2}{\alpha_s}, \alpha_s^2, \alpha_s \alpha_{\text{EM}}, \alpha_{\text{EM}}^2\right) \\
 &= \langle \vec{Q}_{\epsilon'_K}(\mu)^T \rangle \vec{s}_{\text{NLO}}(\mu) + \mathcal{O}\left(\frac{\alpha_{\text{EM}}^2}{\alpha_s}, \alpha_s^2, \alpha_s \alpha_{\text{EM}}, \alpha_{\text{EM}}^2\right). \tag{4.7}
 \end{aligned}$$

Here we have suppressed the opposite-chirality coefficients \vec{s} and the arguments of $\hat{U}(\mu, \mu_{\text{NP}})$ and $\vec{s}(\mu_{\text{NP}})$ for better readability. This procedure defines $\vec{s}_{\text{NLO}}(\mu)$ as a next-to-leading order quantity, where higher orders have been discarded consistently.

In view of undetermined Wilson coefficients, it is beneficial to arrange the terms above according to the Wilson coefficients evaluated at the new physics scale as

$$\begin{aligned} \langle \vec{Q}_{e'_K}(\mu)^T \rangle \vec{s}(\mu) \stackrel{(\text{NLO})}{=} \langle \vec{Q}_{e'_K}(\mu)^T \rangle \left[\left(\hat{U}_0 + \hat{U}_e + \hat{U}_s + \hat{U}_{se} + \hat{U}_{ee} \right) \vec{s}_0 \right. \\ \left. + \left(\hat{U}_0 + \hat{U}_e + \hat{U}_s \right) \vec{s}_e + \left(\hat{U}_0 + \hat{U}_e \right) \vec{s}_s + \hat{U}_0 \vec{s}_{se} + \hat{U}_0 \vec{s}_{ee} \right], \end{aligned} \quad (4.8)$$

where we have again suppressed \vec{s} and the arguments of $\hat{U}(\mu, \mu_{\text{NP}})$ and $\vec{s}(\mu_{\text{NP}})$. For given numerical values for the hadronic matrix elements at a low scale and with our evolution matrices connecting μ_{NP} with the low scale μ , we can determine the *weights* which multiply the Wilson coefficients $\text{Im}[\vec{s}(\mu_{\text{NP}}) - \vec{s}(\mu_{\text{NP}})]$ in eq. (4.8) for any chosen scale of new physics.

4.3 Evolution matrices at the TeV scale

Above the electroweak scale we observe an approximately logarithmic behavior of the evolution matrix $\hat{U}(\mu, \mu_{\text{NP}})$ in eq. (4.6) with increasing energy scale. This observation allows us to derive an approximation for the evolution matrix in the high energy region, which has an error of only a few percent. We give approximate functions for all components of the evolution matrix linking the new physics scale to the hadronic scale. Cast in the form

$$\hat{U}_{0,e,s,se,ee}(\mu, \mu_{\text{NP}}) = \hat{U}_{1,\text{fit}} + \hat{U}_{2,\text{fit}} \ln \frac{\mu_{\text{NP}}}{1 \text{ TeV}}, \quad (4.9)$$

we combine them in terms of eq. (4.8).

Using the analytic evolution matrices evaluated in section 2 and the next-to-leading order matching matrices $\hat{M}_{c,b,t}$, we obtain

$$\begin{aligned} \hat{U}_0(\mu, \mu_{\text{NP}}) + \hat{U}_e(\mu, \mu_{\text{NP}}) + \hat{U}_s(\mu, \mu_{\text{NP}}) + \hat{U}_{se}(\mu, \mu_{\text{NP}}) + \hat{U}_{ee}(\mu, \mu_{\text{NP}}) \\ \simeq \hat{U}_{0,1,\text{fit}} + \hat{U}_{0,2,\text{fit}} \ln \frac{\mu_{\text{NP}}}{1 \text{ TeV}}, \end{aligned} \quad (4.10)$$

for the $\mathcal{O}(1)$ Wilson coefficients at the μ_{NP} scale, and

$$\hat{U}_0(\mu, \mu_{\text{NP}}) + \hat{U}_e(\mu, \mu_{\text{NP}}) + \hat{U}_s(\mu, \mu_{\text{NP}}) \simeq \hat{U}_{e,1,\text{fit}} + \hat{U}_{e,2,\text{fit}} \ln \frac{\mu_{\text{NP}}}{1 \text{ TeV}}, \quad (4.11)$$

$$\hat{U}_0(\mu, \mu_{\text{NP}}) + \hat{U}_e(\mu, \mu_{\text{NP}}) \simeq \hat{U}_{s,1,\text{fit}} + \hat{U}_{s,2,\text{fit}} \ln \frac{\mu_{\text{NP}}}{1 \text{ TeV}}, \quad (4.12)$$

$$\hat{U}_0(\mu, \mu_{\text{NP}}) \simeq \hat{U}_{se,1,\text{fit}} + \hat{U}_{se,2,\text{fit}} \ln \frac{\mu_{\text{NP}}}{1 \text{ TeV}}, \quad (4.13)$$

for the $\mathcal{O}(\alpha_{\text{EM}}/\alpha_s)$, $\mathcal{O}(\alpha_s)$, $\mathcal{O}(\alpha_{\text{EM}})$ (or $\mathcal{O}(\alpha_{\text{EM}}^2/\alpha_s^2)$) Wilson coefficients at the μ_{NP} scale, respectively. Here $\mu = 1.3 \text{ GeV}$ and $\mu_c = 1.4 \text{ GeV}$ are taken, and the fitting matrices \hat{U}_{fit} are given in appendix B. We find that these approximate evolution matrices are highly accurate in the range of 500 GeV–10 TeV.

In order to estimate which Wilson coefficients are expected to gain large enhancements through the RG evolution, we calculate *weights* for the Wilson coefficients at the μ_{NP} scale. We regard the coefficients of $\langle \vec{Q}_{\epsilon'_K}(\mu)^T \rangle \sum_i \hat{U}_i(\mu, \mu_{\text{NP}}) (\vec{s}(\mu_{\text{NP}}) - \vec{s}(\mu_{\text{NP}}))$ in eq. (4.8) as weights of the Wilson coefficients.

In table 3, we list the coefficient $\langle \vec{Q}_{\epsilon'_K}(\mu)^T \rangle (\hat{U}_0 + \hat{U}_e + \hat{U}_s + \hat{U}_{se} + \hat{U}_{ee})$ for the $\mathcal{O}(1)$ Wilson coefficients at the scale $\mu_{\text{NP}} = 1, 3, 5$ and 10 TeV in units of $(\text{GeV})^3$, where the hadronic matrix elements of table 2 are taken. Similarly, the weights of the $\mathcal{O}(\alpha_{\text{EM}}/\alpha_s)$, $\mathcal{O}(\alpha_s)$, and $\mathcal{O}(\alpha_{\text{EM}})$ (or $\mathcal{O}(\alpha_{\text{EM}}^2/\alpha_s^2)$) Wilson coefficients are given in tables 4, 5, and 6, respectively. Note that these values are not obtained by fitting but using the exact analytic evolution matrices. We observe that these values are of course dominated by \hat{U}_0 , with the sub-dominant contribution stemming from \hat{U}_e because of the $1/\omega_+$ enhancement and \hat{U}_s . We also find, that the largest weights come in the 7 and 8 components, and they are further enhanced through the RG evolution in the high energy regime. Compared with the coefficients at the weak scale,

$$\begin{aligned} & \langle \vec{Q}_{\epsilon'_K}(\mu)^T \rangle \hat{U}_0(\mu, M_W) \\ &= (0.37, -0.02, 0.12, -0.29, 0.34, 0.83, 15.33, 54.09, 0.53, 0.08), \end{aligned} \quad (4.14)$$

$$\begin{aligned} & \langle \vec{Q}_{\epsilon'_K}(\mu)^T \rangle (\hat{U}_0 + \hat{U}_e + \hat{U}_s + \hat{U}_{se} + \hat{U}_{ee}) (\mu, 1 \text{ TeV}) \\ &= (0.27, -0.06, 0.05, -0.19, 0.08, 0.31, 26.16, 88.61, 0.12, -0.08), \end{aligned} \quad (4.15)$$

$$\begin{aligned} & \langle \vec{Q}_{\epsilon'_K}(\mu)^T \rangle (\hat{U}_0 + \hat{U}_e + \hat{U}_s + \hat{U}_{se} + \hat{U}_{ee}) (\mu, 10 \text{ TeV}) \\ &= (0.20, -0.11, -0.04, -0.15, -0.15, -0.08, 34.19, 113.60, -0.20, -0.22), \end{aligned} \quad (4.16)$$

the weights of the 7 and 8 components increase by 50–100% through the RG evolution at the scale of 1–10 TeV. If one omits the NLO correction $\hat{U}_e + \dots \hat{U}_{ee}$ in eq. (4.15), one finds 22.77 and 76.05 for the 7th and 8th element (see table 6), which shows the impact of the NLO corrections on these elements. Although the enhancement factor from the RG evolution has been pointed out before in refs. [58, 60] within a leading-order analysis, it has not been considered in most of the literature. We emphasize that this factor should be included when one studies TeV-scale new-physics contributions to the QED-penguin operators in order to alleviate the ϵ'_K/ϵ_K discrepancy.

5 Conclusions and discussion

Based on the first complete lattice calculation of the hadronic matrix elements for the $K \rightarrow \pi\pi$ decay, we have evaluated the Standard-Model prediction of ϵ'_K/ϵ_K at the next-to-leading order. It is well known that the analytic RG evolution matrices for the $\Delta S = 1$ nonleptonic effective Hamiltonian at the next-to-leading order contains singularities in intermediate steps of the calculation. These singularities make practical calculation laborious even though appropriate regulators disappear from the final (physical) result. In this paper, we have generalized the analytic ansatz of the Roma group [11, 21] to solve the RG equations and derive a singularity-free solution by adding logarithmic terms to the ansatz.

Coefficients	$\langle \vec{Q}_{e'_K}(\mu)^T \rangle (\hat{U}_0 + \hat{U}_e + \hat{U}_s + \hat{U}_{se} + \hat{U}_{ee})$			
	μ_{NP} [TeV]	1	3	5
$s_{0,1} - \tilde{s}_{0,1}$	0.265	0.236	0.221	0.199
$s_{0,2} - \tilde{s}_{0,2}$	-0.062	-0.085	-0.095	-0.108
$s_{0,3} - \tilde{s}_{0,3}$	0.045	0.006	-0.014	-0.044
$s_{0,4} - \tilde{s}_{0,4}$	-0.193	-0.178	-0.168	-0.153
$s_{0,5} - \tilde{s}_{0,5}$	0.081	-0.016	-0.067	-0.145
$s_{0,6} - \tilde{s}_{0,6}$	0.305	0.147	0.058	-0.076
$s_{0,7} - \tilde{s}_{0,7}$	26.16	29.97	31.76	34.19
$s_{0,8} - \tilde{s}_{0,8}$	88.61	100.46	106.02	113.60
$s_{0,9} - \tilde{s}_{0,9}$	0.117	-0.024	-0.097	-0.201
$s_{0,10} - \tilde{s}_{0,10}$	-0.084	-0.147	-0.177	-0.219

Table 3. The coefficient $\langle \vec{Q}_{e'_K}(\mu)^T \rangle (\hat{U}_0 + \hat{U}_e + \hat{U}_s + \hat{U}_{se} + \hat{U}_{ee})$ for the $\mathcal{O}(1)$ Wilson coefficients at the scale μ_{NP} in units of $(\text{GeV})^3$, where $\mu = 1.3 \text{ GeV}$.

Coefficients	$\langle \vec{Q}_{e'_K}(\mu)^T \rangle (\hat{U}_0 + \hat{U}_e + \hat{U}_s)$			
	μ_{NP} [TeV]	1	3	5
$s_{e,1} - \tilde{s}_{e,1}$	0.290	0.267	0.255	0.237
$s_{e,2} - \tilde{s}_{e,2}$	-0.076	-0.101	-0.112	-0.127
$s_{e,3} - \tilde{s}_{e,3}$	0.090	0.065	0.051	0.030
$s_{e,4} - \tilde{s}_{e,4}$	-0.234	-0.228	-0.222	-0.213
$s_{e,5} - \tilde{s}_{e,5}$	0.144	0.066	0.023	-0.042
$s_{e,6} - \tilde{s}_{e,6}$	0.423	0.301	0.230	0.120
$s_{e,7} - \tilde{s}_{e,7}$	26.29	30.14	31.93	34.38
$s_{e,8} - \tilde{s}_{e,8}$	88.77	100.67	106.24	113.85
$s_{e,9} - \tilde{s}_{e,9}$	0.216	0.101	0.041	-0.045
$s_{e,10} - \tilde{s}_{e,10}$	-0.096	-0.162	-0.193	-0.236

Table 4. The coefficient $\langle \vec{Q}_{e'_K}(\mu)^T \rangle (\hat{U}_0 + \hat{U}_e + \hat{U}_s)$ for the $\mathcal{O}(\alpha_{\text{EM}}/\alpha_s)$ Wilson coefficients at the scale μ_{NP} in units of $(\text{GeV})^3$, where $\mu = 1.3 \text{ GeV}$.

As a novel feature of our solution compared to refs. [22, 25] we do neither require the diagonalization of the LO anomalous dimension matrix nor case-by-case implementations for different eigenvalues of this matrix. Instead, the different cases are encoded in the \hat{J} matrices given in eqs. (2.30)–(2.38) and appendix A. The singular nature of the RG equations leads to the presence of spurious parameters which cancel between the high-scale

Coefficients μ_{NP} [TeV]	$\langle \vec{Q}_{\epsilon'_K}(\mu)^T \rangle (\hat{U}_0 + \hat{U}_e)$			
	1	3	5	10
$s_{s,1} - \tilde{s}_{s,1}$	0.288	0.266	0.254	0.236
$s_{s,2} - \tilde{s}_{s,2}$	-0.086	-0.111	-0.122	-0.136
$s_{s,3} - \tilde{s}_{s,3}$	0.096	0.071	0.058	0.037
$s_{s,4} - \tilde{s}_{s,4}$	-0.219	-0.208	-0.200	-0.188
$s_{s,5} - \tilde{s}_{s,5}$	0.091	0.004	-0.043	-0.113
$s_{s,6} - \tilde{s}_{s,6}$	0.264	0.119	0.038	-0.086
$s_{s,7} - \tilde{s}_{s,7}$	22.30	25.42	26.88	28.86
$s_{s,8} - \tilde{s}_{s,8}$	75.45	85.00	89.47	95.57
$s_{s,9} - \tilde{s}_{s,9}$	0.208	0.092	0.032	-0.055
$s_{s,10} - \tilde{s}_{s,10}$	-0.108	-0.173	-0.204	-0.246

Table 5. The coefficient $\langle \vec{Q}_{\epsilon'_K}(\mu)^T \rangle (\hat{U}_0 + \hat{U}_e)$ for the $\mathcal{O}(\alpha_s)$ Wilson coefficients at the scale μ_{NP} in units of $(\text{GeV})^3$, where $\mu = 1.3 \text{ GeV}$.

Coefficients μ_{NP} [TeV]	$\langle \vec{Q}_{\epsilon'_K}(\mu)^T \rangle \hat{U}_0$			
	1	3	5	10
$s_{se,1} - \tilde{s}_{se,1}$	0.391	0.401	0.406	0.412
$s_{se,2} - \tilde{s}_{se,2}$	-0.075	-0.098	-0.108	-0.121
$s_{se,3} - \tilde{s}_{se,3}$	0.154	0.167	0.173	0.181
$s_{se,4} - \tilde{s}_{se,4}$	-0.356	-0.387	-0.402	-0.421
$s_{se,5} - \tilde{s}_{se,5}$	0.448	0.495	0.517	0.546
$s_{se,6} - \tilde{s}_{se,6}$	1.126	1.251	1.309	1.388
$s_{se,7} - \tilde{s}_{se,7}$	22.77	26.06	27.60	29.70
$s_{se,8} - \tilde{s}_{se,8}$	76.05	85.80	90.38	96.62
$s_{se,9} - \tilde{s}_{se,9}$	0.556	0.568	0.574	0.582
$s_{se,10} - \tilde{s}_{se,10}$	0.004	-0.027	-0.040	-0.058

Table 6. The coefficient $\langle \vec{Q}_{\epsilon'_K}(\mu)^T \rangle \hat{U}_0$ for the $\mathcal{O}(\alpha_{\text{EM}})$ and $\mathcal{O}(\alpha_{\text{EM}}^2/\alpha_s^2)$ Wilson coefficients at the scale μ_{NP} in units of $(\text{GeV})^3$, where $\mu = 1.3 \text{ GeV}$.

and low-scale NLO terms in the RG evolution matrix and thereby do not produce any ambiguity and play the role of scheme parameters with respect to the regularization of the singularities. Thus we have explicitly proven that all singularities are automatically treated in the proper way without the need for a manual regularization of the evolution matrix. This feature also leads to a subtlety whenever the NLO evolution matrix is com-

binned with LO initial conditions for the Wilson coefficients, as one usually does in studies of new-physics contributions to ϵ'_K .

Using the improved RG evolution matrices and applying the recent lattice results, we have calculated ϵ'_K/ϵ_K in the Standard Model at the next-to-leading order. Our final result is $\epsilon'_K/\epsilon_K = (1.06 \pm 5.07) \times 10^{-4}$, which is 2.8σ below the measured value. Our result is consistent with the recent literature and highlights a tension between the Standard-Model prediction and experiment. The uncertainty is dominated by the lattice result of $\langle(\pi\pi)_0|Q_6|K^0\rangle$. Therefore, upcoming improvements of lattice calculations will reveal whether this tension really calls for new physics or not.

We have also evaluated the evolution matrices in the high energy region for calculations of new physics contributions to ϵ'_K/ϵ_K . To this end we have further obtained an easy-to-use approximate formula for the RG evolution matrices in the TeV region at the next-to-leading order and have also calculated the weights for each of the Wilson coefficients at the scale of new physics. We observe that the largest weights come in the 7 and 8 components of the Wilson coefficients and that they are further enhanced through the RG evolution between electroweak and TeV scales. Here we confirm the feature noticed at LO in refs. [58, 60] and find a further enhancement by the NLO corrections to the evolution matrices. Especially the Wilson coefficients of the QED-penguin operators at the scale of 1–10 TeV increase by 50–100% compared with the Wilson coefficients at the weak scale.

Acknowledgments

The authors thank Andrzej Buras and Chris Sachrajda for illuminating discussions and Christoph Bobeth for pointing our attention to ref. [22]. We are grateful to Andrzej Buras, Martin Gorbahn, and Sebastian Jäger for alerting us to a mistake in an earlier version of this paper. We thank the referee for guiding us to a simpler version of eq. (2.14) and eqs. (2.25)–(2.27) and for pointing out the issue of the running of α_{EM} . The work of UN is supported by BMBF under grant no. 05H15VKKB1. PT acknowledges support from the DFG-funded doctoral school *KSETA*.

A Solutions for the matrices \hat{J}

In this appendix, we summarize the solutions for the matrices \hat{J} of eqs. (2.21)–(2.29). Here we set all arbitrary parameters to be zero, which does not affect the evolution matrix in eq. (2.39). We find that the matrices $\hat{J}_{s,1}$, $\hat{J}_{e,1}$, $\hat{J}_{se,2}$ and $\hat{J}_{ee,1}$ are zero matrices in the case where the active number of flavours is four, five or six.

In the case of four active quark and three active lepton flavors, the matrices \hat{J} are given as follows:

$$\hat{J}_{s,0} = \begin{pmatrix} -0.05587 & 1.848 & 0 & 0 & 0 & 0 & 0 & 0 & 0 & 0 \\ 1.848 & -0.05587 & 0 & 0 & 0 & 0 & 0 & 0 & 0 & 0 \\ -0.9365 & -0.4668 & -4.736 & -2.337 & 0.003212 & 0.3418 & 0.0008031 & 0.08546 & -0.4697 & 0.3586 \\ 0.5649 & -0.07649 & 3.954 & 2.101 & 2.963 & -0.1944 & 0.7408 & -0.04860 & 0.6414 & -0.3081 \\ 0.4272 & 0.3745 & 2.458 & 1.908 & -3.758 & 2.824 & -0.6655 & 0.01002 & 0.05269 & -0.1638 \\ -1.279 & -1.705 & -8.527 & -8.045 & -11.11 & 5.288 & -5.422 & -0.3542 & 0.4257 & -0.09234 \\ 0 & 0 & 0 & 0 & 0 & 0 & -1.096 & 2.784 & 0 & 0 \\ 0 & 0 & 0 & 0 & 0 & 0 & 10.58 & 6.705 & 0 & 0 \\ 0 & 0 & 0 & 0 & 0 & 0 & 0 & 0 & -0.05587 & 1.848 \\ 0 & 0 & 0 & 0 & 0 & 0 & 0 & 0 & 1.848 & -0.05587 \end{pmatrix}, \quad (\text{A.1})$$

$$\hat{J}_{e,0} = \begin{pmatrix} -0.16 & 0 & 0 & 0 & 0 & 0 & 0 & 0 & 0 & 0 & 0 \\ 0 & -0.16 & 0 & 0 & 0 & 0 & 0 & 0 & 0 & 0 & 0 \\ 0.003439 & -0.005106 & 0.001425 & -0.01567 & 0.03486 & 0.09318 & -0.006889 & -0.02519 & -0.07039 & -0.007484 \\ -0.0005069 & -0.01002 & 0.006128 & -0.01290 & 0.01379 & 0.05192 & -0.01036 & 0.006656 & -0.004585 & -0.1036 \\ 0.005392 & -0.006428 & -0.002926 & -0.02657 & 0.07003 & 0.1814 & 0.1252 & 0.1139 & 0.01764 & -0.006001 \\ -0.003848 & -0.0005921 & 0.003105 & 0.009616 & -0.03212 & -0.07626 & -0.01869 & 0.05272 & -0.01310 & -0.006584 \\ 0.1939 & -0.1130 & 0.1686 & -0.4453 & 1.036 & 2.138 & 0.1791 & -0.4654 & 0.4974 & -0.1164 \\ -0.04539 & 0.03811 & -0.04301 & 0.1240 & -0.2759 & -0.5575 & 0.01411 & 0.2606 & -0.1147 & 0.05233 \\ 0.1096 & 0.02356 & -0.01178 & -0.02391 & -0.1192 & -0.5136 & 0.1171 & -0.2515 & 0.1747 & 0.08262 \\ 0.03175 & 0.02141 & 0.08054 & -0.1001 & -0.1933 & -0.5465 & -0.08608 & -0.4136 & 0.05499 & -0.04569 \end{pmatrix}, \quad (\text{A.2})$$

$$\hat{J}_{se,0} = \begin{pmatrix} 0.375 & 1.125 & 0 & 0 & 0 & 0 & 0 & 0 & 0 & 0 \\ -1.125 & -0.375 & 0 & 0 & 0 & 0 & 0 & 0 & 0 & 0 \\ -6.983 & 4.245 & -14.00 & 8.408 & 3.891 & 5.925 & 15.05 & 0.5512 & -13.32 & 8.650 \\ 4.789 & -6.528 & 14.16 & -7.925 & -4.057 & -6.102 & 5.913 & -0.09229 & 6.279 & -15.36 \\ 5.844 & 4.699 & 22.01 & 19.72 & 86.73 & -2.892 & 121.9 & -0.9073 & 6.526 & 4.236 \\ -1.550 & -2.109 & -6.160 & -7.277 & -27.45 & 1.337 & -42.88 & -8.161 & -1.571 & -2.688 \\ -16.91 & -11.78 & -84.30 & -74.62 & -347.6 & 11.87 & -86.80 & 3.237 & -5.914 & 2.873 \\ 4.544 & 3.345 & 26.74 & 24.34 & 110.6 & -6.837 & 26.53 & -1.799 & 0.2636 & -2.134 \\ 7.741 & -3.157 & 27.85 & 6.262 & -0.2248 & -5.260 & -0.06204 & -1.963 & 11.01 & -11.03 \\ -3.806 & 7.758 & -3.113 & 20.22 & 8.580 & 7.661 & 2.683 & 3.178 & -11.43 & 11.46 \end{pmatrix}, \quad (\text{A.3})$$

$$\hat{J}_{se,1} = \begin{pmatrix} -1.437 & -0.3260 & 0 & 0 & 0 & 0 & 0 & 0 & 0 & 0 \\ -0.3260 & -1.437 & 0 & 0 & 0 & 0 & 0 & 0 & 0 & 0 \\ -0.1961 & 0.4893 & -0.6832 & 0.6795 & 0.2602 & 0.1364 & 0.06504 & 0.03410 & -0.9651 & 0.9651 \\ 0.5214 & -0.09977 & 1.000 & -0.2338 & -0.05872 & -0.01202 & -0.01468 & -0.003004 & 0.9009 & -0.9009 \\ 0.05525 & 0.004740 & 0.2305 & 0.1295 & 1.006 & -0.09577 & 0.06746 & -0.02394 & 0.05052 & -0.05052 \\ 0.01468 & 0.006783 & 0.07229 & 0.05649 & -0.7178 & -0.8597 & -0.08158 & -0.1054 & 0.007898 & -0.007898 \\ 0 & 0 & 0 & 0 & 0 & 0 & 0.7365 & 0 & 0 & 0 \\ 0 & 0 & 0 & 0 & 0 & 0 & -0.3915 & -0.4379 & 0 & 0 \\ 0.4798 & -0.07969 & 0 & 0 & 0 & 0 & 0 & 0 & 0.002400 & -0.5651 \\ -0.07969 & 0.4798 & 0 & 0 & 0 & 0 & 0 & 0 & -0.5651 & 0.002400 \end{pmatrix}, \quad (\text{A.4})$$

$$\hat{J}_{ee,0} = \begin{pmatrix} 0.09387 & 0 & 0 & 0 & 0 & 0 & 0 & 0 & 0 & 0 & 0 \\ 0 & 0.09387 & 0 & 0 & 0 & 0 & 0 & 0 & 0 & 0 & 0 \\ -0.007568 & 0.004171 & -0.003074 & 0.01400 & -0.02073 & -0.04983 & 0.009393 & 0.05187 & 0.02577 & 0.005510 & 0.005510 \\ -0.003805 & 0.008022 & -0.01301 & 0.01704 & -0.002762 & -0.01491 & 0.02298 & 0.05596 & -0.004908 & 0.06248 & 0.06248 \\ 0.006342 & -0.003123 & 0.01278 & -0.006150 & 0.002694 & -0.01347 & -0.08904 & -0.1721 & 0.01264 & -0.006294 & -0.006294 \\ -0.001112 & 0.003255 & -0.006809 & 0.001925 & 0.007354 & 0.02220 & 0.02320 & 0.02432 & 0.000069 & 0.008803 & 0.008803 \\ -0.08221 & 0.08779 & -0.06815 & 0.2718 & -0.6678 & -1.605 & 0.02205 & 0.3006 & -0.2125 & 0.1274 & 0.1274 \\ 0.02919 & -0.03213 & 0.02574 & -0.09691 & 0.2203 & 0.5159 & -0.02866 & -0.1783 & 0.07471 & -0.04794 & -0.04794 \\ -0.02286 & -0.03780 & 0.01157 & -0.1058 & 0.3251 & 0.8688 & 0.02406 & 0.1580 & 0.01950 & -0.06052 & -0.06052 \\ -0.01653 & -0.02727 & -0.06727 & -0.001290 & 0.2567 & 0.6911 & 0.1135 & 0.4163 & -0.01594 & 0.01271 & 0.01271 \end{pmatrix}. \quad (\text{A.5})$$

In the case of five active flavours, the matrices \hat{J} are given as follows:

$$\hat{J}_{s,0} = \begin{pmatrix} 0.09940 & 1.528 & 0 & 0 & 0 & 0 & 0 & 0 & 0 & 0 \\ 1.528 & 0.09940 & 0 & 0 & 0 & 0 & 0 & 0 & 0 & 0 \\ -0.8769 & -0.5324 & -5.350 & -3.443 & 6.908 & 0.01534 & 0.6908 & 0.001534 & 0.09398 & 0.5551 \\ 0.3241 & -0.2016 & 2.745 & 1.406 & -5.349 & 0.05042 & -0.5349 & 0.005042 & 0.3637 & -0.2583 \\ 0.5565 & 0.5109 & 3.804 & 3.112 & -3.433 & 2.928 & -0.2259 & 0.01534 & -0.2326 & -0.3566 \\ 0.1455 & -0.6772 & -0.6268 & -1.428 & 13.75 & 4.877 & 0.5228 & -0.3080 & 0.7500 & -0.3175 \\ 0 & 0 & 0 & 0 & 0 & 0 & -1.174 & 2.775 & 0 & 0 \\ 0 & 0 & 0 & 0 & 0 & 0 & 8.519 & 7.957 & 0 & 0 \\ 0 & 0 & 0 & 0 & 0 & 0 & 0 & 0 & 0.09940 & 1.528 \\ 0 & 0 & 0 & 0 & 0 & 0 & 0 & 0 & 1.528 & 0.09940 \end{pmatrix}, \quad (\text{A.6})$$

$$\hat{J}_{e,0} = \begin{pmatrix} -0.1739 & 0 & 0 & 0 & 0 & 0 & 0 & 0 & 0 & 0 \\ 0 & -0.1739 & 0 & 0 & 0 & 0 & 0 & 0 & 0 & 0 \\ -0.00008430 & 0.001850 & 0.0008760 & 0.006336 & -0.01477 & -0.03845 & -0.01774 & -0.05406 & -0.08765 & 0.002382 \\ -0.004461 & -0.006971 & 0.008984 & 0.0005819 & -0.009264 & -0.01468 & -0.01741 & 0.004557 & -0.01788 & -0.1082 \\ 0.005095 & -0.003528 & -0.0004455 & -0.02594 & 0.05269 & 0.1345 & 0.1129 & 0.05212 & 0.01551 & 0.002383 \\ -0.004149 & -0.003101 & 0.003889 & 0.006674 & -0.01610 & -0.03635 & -0.01215 & 0.08836 & -0.01439 & -0.01264 \\ 0.1078 & 0.09271 & 0.04484 & 0.3330 & -0.6222 & -2.183 & 0.08561 & -0.8183 & 0.3009 & 0.1117 \\ -0.01577 & -0.03068 & -0.01027 & -0.1407 & 0.2713 & 0.8851 & 0.05531 & 0.3929 & -0.04218 & -0.02168 \\ 0.1440 & -0.01065 & -0.09022 & -0.05549 & -0.06738 & -0.2646 & 0.2167 & -0.08880 & 0.3031 & -0.004212 \\ 0.06094 & -0.01177 & 0.04954 & -0.1338 & -0.1006 & -0.2569 & -0.02778 & -0.3062 & 0.1580 & -0.1423 \end{pmatrix}, \quad (\text{A.7})$$

$$\hat{J}_{se,0} = \begin{pmatrix} 0.375 & 1.125 & 0 & 0 & 0 & 0 & 0 & 0 & 0 & 0 \\ -1.125 & -0.375 & 0 & 0 & 0 & 0 & 0 & 0 & 0 & 0 \\ -2.500 & 1.4315 & -3.851 & 2.898 & 0.9962 & 2.635 & 10.87 & -0.1166 & -5.228 & 3.122 \\ 1.642 & -2.134 & 4.912 & -1.460 & -1.726 & -2.608 & 6.969 & 0.4229 & 1.620 & -5.702 \\ 2.180 & 1.968 & 3.317 & 2.955 & 13.61 & -0.6743 & 69.30 & -0.1624 & 4.882 & 4.428 \\ -0.6997 & -1.109 & -0.9273 & -0.8342 & -4.444 & 0.3460 & -27.91 & -5.246 & -1.635 & -2.910 \\ -6.153 & -3.916 & -35.13 & -28.90 & -136.4 & 5.962 & -13.59 & 0.7483 & 1.775 & 3.592 \\ 1.549 & 0.8194 & 12.28 & 9.893 & 45.61 & -3.670 & 3.698 & -0.4178 & -1.493 & -2.488 \\ 3.019 & -0.8036 & 16.92 & 5.807 & -9.717 & -3.182 & -1.440 & -1.383 & 2.308 & -3.745 \\ -1.305 & 3.483 & -3.346 & 11.38 & -1.864 & 6.249 & 0.2816 & 2.227 & -3.812 & 3.052 \end{pmatrix}, \quad (\text{A.8})$$

$$\hat{J}_{se,1} = \begin{pmatrix} -1.361 & -0.3748 & 0 & 0 & 0 & 0 & 0 & 0 & 0 & 0 \\ -0.3748 & -1.361 & 0 & 0 & 0 & 0 & 0 & 0 & 0 & 0 \\ 0.1224 & 0.1600 & -0.3109 & 0.4207 & 0.1276 & 0.1172 & 0.01276 & 0.01172 & -0.1577 & 0.08237 \\ 0.1835 & 0.1929 & 0.6790 & 0.08838 & -0.09612 & 0.000429 & -0.009612 & 0.000043 & 0.02365 & -0.1460 \\ 0.01271 & -0.01502 & 0.03352 & -0.04966 & 0.3448 & -0.06405 & -0.07195 & -0.006405 & 0.02137 & -0.02022 \\ 0.01922 & 0.01290 & 0.1219 & 0.1030 & -0.3008 & -0.3655 & 0.03423 & 0.04996 & -0.003290 & -0.01277 \\ 0 & 0 & 0 & 0 & 0 & 0 & 1.064 & 0 & 0 & 0 \\ 0 & 0 & 0 & 0 & 0 & 0 & -0.6431 & -0.8651 & 0 & 0 \\ 0.2542 & 0.009287 & 0 & 0 & 0 & 0 & 0 & 0 & -0.5983 & -0.3469 \\ 0.009287 & 0.2542 & 0 & 0 & 0 & 0 & 0 & 0 & -0.3469 & -0.5983 \end{pmatrix}, \quad (\text{A.9})$$

$$\hat{J}_{ee,0} = \begin{pmatrix} 0.1159 & 0 & 0 & 0 & 0 & 0 & 0 & 0 & 0 & 0 \\ 0 & 0.1159 & 0 & 0 & 0 & 0 & 0 & 0 & 0 & 0 \\ -0.006758 & -0.000220 & 0.001054 & -0.007266 & 0.02571 & 0.06903 & 0.01810 & 0.08137 & 0.03717 & 0.002972 \\ -0.001817 & 0.005815 & -0.01259 & -0.005803 & 0.04023 & 0.09858 & 0.03282 & 0.07166 & 0.000845 & 0.07832 \\ -0.001142 & 0.01273 & 0.001550 & 0.06754 & -0.1345 & -0.3735 & -0.09641 & -0.1631 & -0.004201 & 0.004407 \\ 0.002002 & -0.001365 & -0.003840 & -0.02566 & 0.05563 & 0.1504 & 0.02425 & 0.009857 & 0.007927 & 0.008735 \\ -0.007347 & -0.07684 & -0.01964 & -0.3217 & 0.5632 & 1.675 & 0.1525 & 0.6839 & -0.01222 & -0.06966 \\ 0.002651 & 0.02899 & 0.004425 & 0.1344 & -0.2542 & -0.7479 & -0.07896 & -0.3310 & 0.005741 & 0.01977 \\ -0.07157 & 0.03534 & 0.03101 & 0.08707 & -0.08769 & -0.2702 & -0.06562 & -0.03941 & -0.1143 & 0.06248 \\ -0.05563 & 0.02067 & -0.05241 & 0.08527 & 0.06749 & 0.1530 & 0.06268 & 0.3315 & -0.1407 & 0.1353 \end{pmatrix}. \quad (\text{A.10})$$

Above the scale M_W in the $f = 5$ case only $\hat{J}_{ee,0}$ is replaced by

$$\hat{J}_{ee,0} = \begin{pmatrix} 0.1020 & 0 & 0 & 0 & 0 & 0 & 0 & 0 & 0 & 0 \\ 0 & 0.1020 & 0 & 0 & 0 & 0 & 0 & 0 & 0 & 0 \\ -0.006807 & 0.000021 & 0.001232 & -0.006242 & 0.02332 & 0.06286 & 0.01511 & 0.07266 & 0.02996 & 0.003183 \\ -0.002382 & 0.005057 & -0.01143 & -0.005667 & 0.03882 & 0.09606 & 0.03033 & 0.07109 & -0.001430 & 0.06900 \\ -0.000380 & 0.01202 & 0.001590 & 0.06336 & -0.1261 & -0.3519 & -0.08537 & -0.1542 & -0.001936 & 0.004376 \\ 0.001464 & -0.001586 & -0.003427 & -0.02457 & 0.05312 & 0.1445 & 0.02260 & 0.01625 & 0.006104 & 0.007528 \\ -0.000419 & -0.06346 & -0.01667 & -0.2598 & 0.4436 & 1.319 & 0.1296 & 0.5317 & 0.007078 & -0.06051 \\ 0.001486 & 0.02427 & 0.003764 & 0.1115 & -0.2096 & -0.6173 & -0.06592 & -0.2708 & 0.002577 & 0.01708 \\ -0.05788 & 0.03230 & 0.02696 & 0.08653 & -0.1037 & -0.3173 & -0.05763 & -0.07181 & -0.08512 & 0.05362 \\ -0.04767 & 0.01862 & -0.04578 & 0.07839 & 0.04976 & 0.1078 & 0.05242 & 0.2757 & -0.1201 & 0.1187 \end{pmatrix}. \quad (\text{A.11})$$

In the case of six active flavours, the matrices \hat{J} are given as follows:

$$\hat{J}_{s,0} = \begin{pmatrix} 0.3146 & 1.056 & 0 & 0 & 0 & 0 & 0 & 0 & 0 & 0 \\ 1.056 & 0.3146 & 0 & 0 & 0 & 0 & 0 & 0 & 0 & 0 \\ -1.600 & -1.535 & -12.36 & -12.02 & 8.793 & -1.131 & 2.198 & -0.2828 & -0.8657 & -0.8686 \\ 0.8862 & 0.5280 & 7.429 & 7.255 & -5.576 & 0.6539 & -1.394 & 0.1635 & 0.8013 & 0.4058 \\ 0.6905 & 0.7180 & 5.579 & 5.023 & -4.997 & 3.346 & -0.9249 & 0.1452 & 0.3177 & 0.2199 \\ 0.1455 & -0.6299 & -0.3870 & -1.489 & 7.913 & 5.885 & -0.09758 & -0.9513 & 0.8482 & -0.5904 \\ 0 & 0 & 0 & 0 & 0 & 0 & -1.298 & 2.766 & 0 & 0 \\ 0 & 0 & 0 & 0 & 0 & 0 & 8.303 & 9.690 & 0 & 0 \\ 0 & 0 & 0 & 0 & 0 & 0 & 0 & 0 & 0.3146 & 1.056 \\ 0 & 0 & 0 & 0 & 0 & 0 & 0 & 0 & 1.056 & 0.3146 \end{pmatrix}, \quad (\text{A.12})$$

$$\hat{J}_{e,0} = \begin{pmatrix} -0.1905 & 0 & 0 & 0 & 0 & 0 & 0 & 0 & 0 & 0 & 0 \\ 0 & -0.1905 & 0 & 0 & 0 & 0 & 0 & 0 & 0 & 0 & 0 \\ -0.004325 & 0.007185 & 0.009385 & 0.009390 & -0.02752 & -0.06628 & -0.02694 & -0.07676 & -0.1194 & 0.02764 \\ -0.009919 & -0.002219 & 0.03288 & -0.01917 & -0.02621 & -0.02129 & -0.02834 & 0.01474 & -0.06108 & -0.09564 \\ 0.005509 & -0.002168 & -0.01074 & -0.009225 & 0.03980 & 0.08293 & 0.1274 & 0.05083 & 0.03016 & -0.005145 \\ -0.004879 & -0.003778 & 0.01343 & -0.008532 & -0.01554 & -0.01330 & -0.01789 & 0.1048 & -0.02867 & -0.01273 \\ 0.1518 & 0.04324 & 0.2197 & 0.2298 & -0.1970 & -1.348 & 0.2127 & -0.8371 & 0.5734 & 0.07970 \\ -0.02942 & -0.01451 & -0.04693 & -0.1085 & 0.1550 & 0.6298 & 0.03875 & 0.4193 & -0.1089 & -0.01106 \\ 0.1723 & -0.02276 & 0.05556 & -0.02633 & -0.008854 & -0.3349 & 0.3311 & -0.08373 & 0.5572 & -0.08924 \\ 0.08303 & -0.02141 & 0.1183 & -0.1089 & -0.1361 & -0.3994 & -0.03402 & -0.4332 & 0.3145 & -0.2324 \end{pmatrix}, \quad (\text{A.13})$$

$$\hat{J}_{se,0} = \begin{pmatrix} 0.375 & 1.125 & 0 & 0 & 0 & 0 & 0 & 0 & 0 & 0 \\ -1.125 & -0.375 & 0 & 0 & 0 & 0 & 0 & 0 & 0 & 0 \\ -1.717 & 0.4502 & -4.641 & 1.340 & 1.346 & 3.309 & 6.823 & -0.04493 & -4.718 & 1.585 \\ 1.485 & -0.6824 & 4.572 & -1.354 & -0.9936 & -3.700 & 6.745 & 0.4676 & 3.500 & -2.081 \\ 2.474 & 2.178 & 8.318 & 7.311 & 25.97 & -1.158 & 48.94 & -0.4794 & 6.973 & 6.144 \\ -0.6938 & -0.9269 & -2.447 & -2.263 & -8.583 & 0.05831 & -20.43 & -7.770 & -1.899 & -3.039 \\ -4.430 & -2.583 & -32.52 & -26.58 & -103.8 & 4.885 & -26.00 & 1.075 & 0.3241 & 3.002 \\ 1.087 & 0.2394 & 11.23 & 7.972 & 34.52 & -1.077 & 7.739 & -0.2204 & -0.7237 & -2.909 \\ 1.392 & -0.5260 & 11.12 & 3.336 & -9.094 & -3.990 & -4.493 & -2.786 & 3.083 & -2.243 \\ -0.9953 & 1.721 & -6.237 & 4.523 & -0.8947 & 6.267 & -1.189 & 3.698 & -3.152 & 3.108 \end{pmatrix}, \quad (\text{A.14})$$

$$\hat{J}_{se,1} = \begin{pmatrix} -1.215 & -0.4779 & 0 & 0 & 0 & 0 & 0 & 0 & 0 & 0 \\ -0.4779 & -1.215 & 0 & 0 & 0 & 0 & 0 & 0 & 0 & 0 \\ 0.03954 & 0.1511 & -0.5005 & 0.3909 & 0.2004 & 0.09779 & 0.05009 & 0.02445 & -0.1793 & 0.2458 \\ 0.1726 & 0.1039 & 0.6485 & -0.07127 & -0.05979 & 0.04647 & -0.01495 & 0.01162 & 0.2136 & -0.1041 \\ 0.02675 & -0.003629 & 0.1532 & 0.03172 & 0.4150 & -0.09556 & 0.04074 & -0.02389 & 0.04375 & -0.03219 \\ 0.009964 & 0.01439 & 0.08856 & 0.1063 & -0.4370 & -0.6094 & 0.002421 & 0.1197 & 0.000558 & 0.01162 \\ 0 & 0 & 0 & 0 & 0 & 0 & 0.2520 & 0 & 0 & 0 \\ 0 & 0 & 0 & 0 & 0 & 0 & -0.4467 & -1.088 & 0 & 0 \\ 0.1161 & -0.000709 & 0 & 0 & 0 & 0 & 0 & 0 & -0.6925 & -0.4811 \\ -0.000709 & 0.1161 & 0 & 0 & 0 & 0 & 0 & 0 & -0.4811 & -0.6925 \end{pmatrix}, \quad (\text{A.15})$$

$$\hat{J}_{ec,0} = \begin{pmatrix} 0.1391 & 0 & 0 & 0 & 0 & 0 & 0 & 0 & 0 & 0 \\ 0 & 0.1391 & 0 & 0 & 0 & 0 & 0 & 0 & 0 & 0 \\ -0.003752 & -0.006197 & -0.01666 & -0.01541 & 0.04809 & 0.1273 & 0.03381 & 0.1356 & 0.06098 & -0.02018 \\ 0.000326 & 0.001314 & -0.05390 & 0.004611 & 0.07978 & 0.1672 & 0.06923 & 0.1516 & 0.02842 & 0.07314 \\ 0.002820 & 0.007589 & 0.02592 & 0.04766 & -0.1033 & -0.2861 & -0.1243 & -0.2192 & -0.000268 & 0.01032 \\ -0.000053 & 0.001118 & -0.02262 & -0.01220 & 0.05444 & 0.1313 & 0.04123 & 0.03780 & 0.01107 & 0.01113 \\ -0.004754 & -0.04852 & -0.04424 & -0.2157 & 0.2605 & 0.8907 & 0.1751 & 0.6774 & 0.000729 & -0.1105 \\ 0.009495 & 0.01675 & 0.02216 & 0.1040 & -0.1569 & -0.5103 & -0.08580 & -0.3685 & 0.03165 & 0.02339 \\ -0.06667 & 0.03419 & 0.000002 & 0.06611 & -0.03570 & -0.1442 & -0.07226 & -0.1137 & -0.1609 & 0.1208 \\ -0.07613 & 0.02859 & -0.1156 & 0.05588 & 0.1459 & 0.3689 & 0.1048 & 0.5101 & -0.2848 & 0.2398 \end{pmatrix}. \quad (\text{A.16})$$

B Approximation of evolution matrices

In this appendix we list the approximate evolution matrices \hat{U}_{fit} of eqs. (4.10)–(4.13).

The evolution matrices for the $\mathcal{O}(1)$ Wilson coefficients are

$$\hat{U}_{0,1,\text{fit}} = \begin{pmatrix} 1.381 & -0.6586 & 0 & 0 & 0 & 0 & 0 & 0 & 0 & 0 \\ -0.6579 & 1.383 & 0 & 0 & 0 & 0 & 0 & 0 & 0 & 0 \\ -0.02657 & 0.04460 & 1.347 & -0.5061 & 0.1084 & 0.3509 & 0.01854 & 0.05795 & -0.05577 & 0.05648 \\ 0.03219 & -0.08950 & -0.7163 & 1.076 & -0.1140 & -0.5954 & -0.02081 & -0.1003 & 0.1029 & -0.0863 \\ 0.006732 & 0.009857 & 0.06040 & 0.03421 & 0.8730 & 0.3916 & -0.009192 & 0.006706 & -0.002316 & -0.002685 \\ 0.04266 & -0.1445 & -0.1220 & -0.5808 & 1.196 & 3.844 & -0.04416 & -0.2361 & 0.1676 & -0.1556 \\ -0.006910 & -0.000813 & -0.005331 & 0.005611 & -0.01547 & -0.01260 & 0.8834 & 0.3349 & -0.01980 & -0.006946 \\ -0.006196 & 0.000386 & -0.005099 & 0.009086 & -0.02131 & -0.05363 & 1.377 & 5.070 & -0.02191 & -0.004320 \\ -0.008814 & -0.000827 & 0.005846 & 0.000204 & -0.007655 & -0.005259 & -0.02659 & -0.01518 & 1.348 & -0.6634 \\ 0.002569 & -0.000270 & -0.004176 & 0.01113 & 0.002071 & -0.000822 & 0.008502 & 0.004499 & -0.6453 & 1.377 \end{pmatrix}, \quad (\text{B.1})$$

$$\hat{U}_{0,2,\text{fit}} = \begin{pmatrix} 0.04902 & -0.06578 & 0 & 0 & 0 & 0 & 0 & 0 & 0 & 0 \\ -0.06571 & 0.04921 & 0 & 0 & 0 & 0 & 0 & 0 & 0 & 0 \\ -0.002858 & 0.004911 & 0.04273 & -0.04448 & 0.01743 & 0.06239 & 0.003106 & 0.01145 & -0.005919 & 0.007786 \\ 0.004467 & -0.006409 & -0.05801 & 0.02537 & -0.02718 & -0.09404 & -0.004846 & -0.01681 & 0.008209 & -0.01020 \\ 0.000051 & -0.000773 & 0.000153 & -0.005655 & 0.004400 & 0.04479 & -0.000598 & -0.000873 & 0.001332 & -0.001328 \\ 0.007679 & -0.01904 & -0.001577 & -0.08913 & 0.1533 & 0.3766 & -0.01304 & -0.05873 & 0.02464 & -0.03331 \\ -0.000971 & 0.000008 & -0.001421 & 0.000965 & -0.003372 & -0.003838 & -0.000828 & 0.04034 & -0.003464 & -0.000859 \\ -0.002034 & 0.000038 & -0.002690 & 0.002769 & -0.008055 & -0.01680 & 0.2019 & 0.6221 & -0.008119 & -0.001580 \\ -0.001513 & -0.000057 & 0.000438 & -0.000632 & -0.002303 & -0.001513 & -0.005736 & -0.003896 & 0.04208 & -0.06626 \\ 0.000823 & -0.000001 & -0.000722 & 0.001962 & 0.000930 & -0.000258 & 0.002827 & 0.001194 & -0.06154 & 0.04840 \end{pmatrix}. \quad (\text{B.2})$$

The evolution matrices for the $\mathcal{O}(\alpha_{\text{EM}}/\alpha_s)$ Wilson coefficients are

$$\hat{U}_{e,1,\text{fit}} = \begin{pmatrix} 1.384 & -0.6596 & 0 & 0 & 0 & 0 & 0 & 0 & 0 & 0 \\ -0.6596 & 1.384 & 0 & 0 & 0 & 0 & 0 & 0 & 0 & 0 \\ -0.02644 & 0.04449 & 1.347 & -0.5063 & 0.1084 & 0.3508 & 0.01869 & 0.05786 & -0.05398 & 0.05588 \\ 0.03221 & -0.08918 & -0.7165 & 1.076 & -0.1138 & -0.5947 & -0.02013 & -0.09927 & 0.1027 & -0.08501 \\ 0.006614 & 0.009876 & 0.06024 & 0.03434 & 0.8727 & 0.3913 & -0.01040 & 0.007747 & -0.002679 & -0.002541 \\ 0.04268 & -0.1441 & -0.1221 & -0.5803 & 1.196 & 3.845 & -0.04218 & -0.2321 & 0.1682 & -0.1550 \\ -0.007192 & -0.001077 & -0.005373 & 0.005309 & -0.01602 & -0.005198 & 0.8816 & 0.3370 & -0.0213 & -0.006792 \\ -0.004750 & -0.000363 & -0.002599 & 0.006771 & -0.01759 & -0.04805 & 1.385 & 5.079 & -0.01599 & -0.005018 \\ -0.009682 & -0.001318 & 0.009455 & 0.000347 & -0.008310 & -0.004251 & -0.02899 & -0.01618 & 1.347 & -0.6649 \\ 0.003240 & 0.000337 & -0.006239 & 0.01228 & 0.002650 & -0.000994 & 0.009981 & 0.004416 & -0.6448 & 1.380 \end{pmatrix}, \quad (\text{B.3})$$

$$\hat{U}_{e,2,\text{fit}} = \begin{pmatrix} 0.04959 & -0.06613 & 0 & 0 & 0 & 0 & 0 & 0 & 0 & 0 \\ -0.06613 & 0.04959 & 0 & 0 & 0 & 0 & 0 & 0 & 0 & 0 \\ -0.002814 & 0.004885 & 0.04276 & -0.04452 & 0.01748 & 0.06243 & 0.003194 & 0.01153 & -0.005538 & 0.007572 \\ 0.004455 & -0.006361 & -0.05804 & 0.02537 & -0.02712 & -0.09391 & -0.004734 & -0.01663 & 0.008081 & -0.009949 \\ 0.000025 & -0.000747 & 0.000109 & -0.005599 & 0.004337 & 0.04466 & -0.000661 & -0.000532 & 0.001256 & -0.001236 \\ 0.007654 & -0.01896 & -0.001614 & -0.08899 & 0.1534 & 0.3766 & -0.01270 & -0.05792 & 0.02470 & -0.03318 \\ -0.001020 & -0.000042 & -0.001512 & 0.000625 & -0.002880 & -0.001394 & -0.000771 & 0.04163 & -0.003738 & -0.000825 \\ -0.001700 & -0.000089 & -0.001936 & 0.002320 & -0.007113 & -0.01521 & 0.2036 & 0.6241 & -0.006620 & -0.001725 \\ -0.001794 & -0.000100 & 0.000773 & -0.000779 & -0.002622 & -0.001291 & -0.006709 & -0.004276 & 0.04126 & -0.06661 \\ 0.000955 & 0.000077 & -0.001109 & 0.002185 & 0.001279 & -0.000036 & 0.003500 & 0.001712 & -0.06132 & 0.04896 \end{pmatrix}. \quad (\text{B.4})$$

The evolution matrices for the $\mathcal{O}(\alpha_s)$ Wilson coefficients are

$$\hat{U}_{s,1,\text{fit}} = \begin{pmatrix} 1.411 & -0.7127 & 0 & 0 & 0 & 0 & 0 & 0 & 0 & 0 \\ -0.7127 & 1.411 & 0 & 0 & 0 & 0 & 0 & 0 & 0 & 0 \\ -0.009379 & 0.03849 & 1.428 & -0.5372 & 0.05796 & 0.3276 & 0.009884 & 0.05309 & -0.03652 & 0.03661 \\ 0.01918 & -0.06796 & -0.7546 & 1.116 & -0.1185 & -0.6070 & -0.02120 & -0.1018 & 0.07697 & -0.06536 \\ -0.005195 & 0.01615 & 0.009571 & 0.06192 & 0.8626 & 0.1512 & 0.001064 & 0.02609 & -0.01979 & 0.01784 \\ 0.02719 & -0.1165 & -0.1074 & -0.5139 & 1.020 & 3.416 & -0.03532 & -0.1846 & 0.1343 & -0.1238 \\ -0.007192 & -0.001077 & -0.005373 & 0.005309 & -0.01602 & -0.005198 & 0.8044 & -0.01284 & -0.02130 & -0.006792 \\ -0.004750 & -0.000363 & -0.002599 & 0.006771 & -0.01759 & -0.04805 & 1.166 & 4.362 & -0.01599 & -0.005018 \\ -0.009682 & -0.001318 & 0.009455 & 0.000347 & -0.008310 & -0.004251 & -0.02899 & -0.01618 & 1.373 & -0.7181 \\ 0.003240 & 0.000337 & -0.006239 & 0.01228 & 0.002650 & -0.000994 & 0.009981 & 0.004416 & -0.6980 & 1.406 \end{pmatrix}, \quad (\text{B.5})$$

$$\hat{U}_{s,2,\text{fit}} = \begin{pmatrix} 0.05237 & -0.06874 & 0 & 0 & 0 & 0 & 0 & 0 & 0 & 0 \\ -0.06874 & 0.05237 & 0 & 0 & 0 & 0 & 0 & 0 & 0 & 0 \\ -0.001807 & 0.004179 & 0.04830 & -0.04670 & 0.01449 & 0.05948 & 0.002493 & 0.01111 & -0.003888 & 0.006388 \\ 0.003138 & -0.005261 & -0.06167 & 0.02726 & -0.02594 & -0.09351 & -0.004500 & -0.01681 & 0.006327 & -0.008337 \\ -0.000731 & 0.000706 & -0.001981 & 0.001873 & -0.004333 & 0.01923 & 0.000445 & 0.003261 & -0.001199 & 0.001503 \\ 0.005578 & -0.01553 & -0.002278 & -0.07695 & 0.1317 & 0.3191 & -0.01019 & -0.04632 & 0.01977 & -0.02734 \\ -0.001020 & -0.000042 & -0.001512 & 0.000625 & -0.002880 & -0.001394 & -0.01510 & -0.002932 & -0.003738 & -0.000825 \\ -0.001700 & -0.000089 & -0.001936 & 0.002320 & -0.007113 & -0.01521 & 0.1673 & 0.5064 & -0.006620 & -0.001725 \\ -0.001794 & -0.000100 & 0.000773 & -0.000779 & -0.002622 & -0.001291 & -0.006709 & -0.004276 & 0.04404 & -0.06921 \\ 0.000955 & 0.000077 & -0.001109 & 0.002185 & 0.001279 & -0.000036 & 0.003500 & 0.001712 & -0.06393 & 0.05174 \end{pmatrix}. \quad (\text{B.6})$$

The evolution matrices for the $\mathcal{O}(\alpha_{\text{EM}})$ and $\mathcal{O}(\alpha_{\text{EM}}^2/\alpha_s^2)$ Wilson coefficients are

$$\hat{U}_{se,1,\text{fit}} = \begin{pmatrix} 1.394 & -0.7045 & 0 & 0 & 0 & 0 & 0 & 0 & 0 & 0 \\ -0.7045 & 1.394 & 0 & 0 & 0 & 0 & 0 & 0 & 0 & 0 \\ -0.009453 & 0.03820 & 1.428 & -0.5374 & 0.05790 & 0.3279 & 0.009686 & 0.05425 & -0.04508 & 0.03987 \\ 0.01931 & -0.06738 & -0.7551 & 1.116 & -0.1184 & -0.6078 & -0.02089 & -0.1042 & 0.08184 & -0.07190 \\ -0.005225 & 0.01599 & 0.009690 & 0.06182 & 0.8626 & 0.1514 & 0.005876 & 0.02676 & -0.01998 & 0.01742 \\ 0.02740 & -0.1156 & -0.1079 & -0.5135 & 1.020 & 3.415 & -0.02789 & -0.1626 & 0.1356 & -0.1214 \\ 0 & 0 & 0 & 0 & 0 & 0 & 0.8305 & 0 & 0 & 0 \\ 0 & 0 & 0 & 0 & 0 & 0 & 1.188 & 4.394 & 0 & 0 \\ 0 & 0 & 0 & 0 & 0 & 0 & 0 & 0 & 1.394 & -0.7045 \\ 0 & 0 & 0 & 0 & 0 & 0 & 0 & 0 & -0.7045 & 1.394 \end{pmatrix}, \quad (\text{B.7})$$

$$\hat{U}_{se,2,\text{fit}} = \begin{pmatrix} 0.04914 & -0.06644 & 0 & 0 & 0 & 0 & 0 & 0 & 0 & 0 \\ -0.06644 & 0.04914 & 0 & 0 & 0 & 0 & 0 & 0 & 0 & 0 \\ -0.001818 & 0.004086 & 0.04834 & -0.04679 & 0.01446 & 0.05962 & 0.002471 & 0.01164 & -0.005626 & 0.007251 \\ 0.003145 & -0.005101 & -0.06177 & 0.02741 & -0.02592 & -0.09379 & -0.004515 & -0.01783 & 0.007658 & -0.009488 \\ -0.000730 & 0.000669 & -0.001957 & 0.001837 & -0.004334 & 0.01930 & 0.001106 & 0.003520 & -0.001234 & 0.001403 \\ 0.005619 & -0.01524 & -0.002424 & -0.07670 & 0.1318 & 0.3187 & -0.007642 & -0.03995 & 0.02017 & -0.02644 \\ 0 & 0 & 0 & 0 & 0 & 0 & -0.01058 & 0 & 0 & 0 \\ 0 & 0 & 0 & 0 & 0 & 0 & 0.1759 & 0.5171 & 0 & 0 \\ 0 & 0 & 0 & 0 & 0 & 0 & 0 & 0 & 0.04914 & -0.06644 \\ 0 & 0 & 0 & 0 & 0 & 0 & 0 & 0 & -0.06644 & 0.04914 \end{pmatrix}. \quad (\text{B.8})$$

Open Access. This article is distributed under the terms of the Creative Commons Attribution License ([CC-BY 4.0](https://creativecommons.org/licenses/by/4.0/)), which permits any use, distribution and reproduction in any medium, provided the original author(s) and source are credited.

References

- [1] F.J. Gilman and M.B. Wise, *The $\Delta I = 1/2$ Rule and Violation of CP in the Six Quark Model*, *Phys. Lett.* **B 83** (1979) 83 [[INSPIRE](#)].
- [2] B. Guberina and R.D. Peccei, *Quantum Chromodynamic Effects and CP-violation in the Kobayashi-Maskawa Model*, *Nucl. Phys.* **B 163** (1980) 289 [[INSPIRE](#)].
- [3] J.S. Hagelin and F.J. Gilman, *A lower bound on $|\epsilon'/\epsilon|$* , *Phys. Lett.* **B 126** (1983) 111 [[INSPIRE](#)].
- [4] A.J. Buras and J.M. Gérard, *ϵ'/ϵ in the Standard Model*, *Phys. Lett.* **B 203** (1988) 272 [[INSPIRE](#)].
- [5] J.M. Flynn and L. Randall, *The Electromagnetic Penguin Contribution to ϵ'/ϵ for Large Top Quark Mass*, *Phys. Lett.* **B 224** (1989) 221 [*Erratum ibid.* **B 235** (1990) 412] [[INSPIRE](#)].
- [6] G. Buchalla, A.J. Buras and M.K. Harlander, *The Anatomy of ϵ'/ϵ in the Standard Model*, *Nucl. Phys.* **B 337** (1990) 313 [[INSPIRE](#)].
- [7] E.A. Paschos and Y.L. Wu, *Correlations between ϵ'/ϵ and heavy top*, *Mod. Phys. Lett.* **A 6** (1991) 93 [[INSPIRE](#)].
- [8] M. Lusignoli, L. Maiani, G. Martinelli and L. Reina, *Mixing and CP-violation in K and B mesons: A Lattice QCD point of view*, *Nucl. Phys.* **B 369** (1992) 139 [[INSPIRE](#)].
- [9] A.J. Buras, M. Jamin, M.E. Lautenbacher and P.H. Weisz, *Effective Hamiltonians for $\Delta S = 1$ and $\Delta B = 1$ nonleptonic decays beyond the leading logarithmic approximation*, *Nucl. Phys.* **B 370** (1992) 69 [*Addendum ibid.* **B 375** (1992) 501] [[INSPIRE](#)].
- [10] A.J. Buras, M. Jamin, M.E. Lautenbacher and P.H. Weisz, *Two loop anomalous dimension matrix for $\Delta S = 1$ weak nonleptonic decays I: $\mathcal{O}(\alpha_s^2)$* , *Nucl. Phys.* **B 400** (1993) 37 [[hep-ph/9211304](#)] [[INSPIRE](#)].
- [11] M. Ciuchini, E. Franco, G. Martinelli and L. Reina, *The $\Delta S = 1$ effective Hamiltonian including next-to-leading order QCD and QED corrections*, *Nucl. Phys.* **B 415** (1994) 403 [[hep-ph/9304257](#)] [[INSPIRE](#)].
- [12] A.J. Buras, M. Jamin and M.E. Lautenbacher, *Two loop anomalous dimension matrix for $\Delta S = 1$ weak nonleptonic decays. (II) $\mathcal{O}(\alpha\alpha_s)$* , *Nucl. Phys.* **B 400** (1993) 75 [[hep-ph/9211321](#)] [[INSPIRE](#)].
- [13] A.J. Buras, M. Jamin and M.E. Lautenbacher, *The Anatomy of ϵ'/ϵ beyond leading logarithms with improved hadronic matrix elements*, *Nucl. Phys.* **B 408** (1993) 209 [[hep-ph/9303284](#)] [[INSPIRE](#)].
- [14] A.J. Buras, M. Gorbahn, S. Jäger and M. Jamin, *Improved anatomy of ϵ'/ϵ in the Standard Model*, *JHEP* **11** (2015) 202 [[arXiv:1507.06345](#)] [[INSPIRE](#)].
- [15] V. Cirigliano, A. Pich, G. Ecker and H. Neufeld, *Isospin violation in ϵ'* , *Phys. Rev. Lett.* **91** (2003) 162001 [[hep-ph/0307030](#)] [[INSPIRE](#)].
- [16] V. Cirigliano, G. Ecker, H. Neufeld and A. Pich, *Isospin breaking in $K \rightarrow \pi\pi$ decays*, *Eur. Phys. J. C* **33** (2004) 369 [[hep-ph/0310351](#)] [[INSPIRE](#)].

- [17] T. Blum et al., *The $K \rightarrow (\pi\pi)_{I=2}$ Decay Amplitude from Lattice QCD*, *Phys. Rev. Lett.* **108** (2012) 141601 [[arXiv:1111.1699](#)] [[INSPIRE](#)].
- [18] T. Blum et al., *Lattice determination of the $K \rightarrow (\pi\pi)_{I=2}$ Decay Amplitude A_2* , *Phys. Rev. D* **86** (2012) 074513 [[arXiv:1206.5142](#)] [[INSPIRE](#)].
- [19] T. Blum et al., *$K \rightarrow \pi\pi$ $\Delta I = 3/2$ decay amplitude in the continuum limit*, *Phys. Rev. D* **91** (2015) 074502 [[arXiv:1502.00263](#)] [[INSPIRE](#)].
- [20] RBC/UKQCD collaboration, Z. Bai et al., *Standard Model Prediction for Direct CP-violation in $K \rightarrow \pi\pi$ Decay*, *Phys. Rev. Lett.* **115** (2015) 212001 [[arXiv:1505.07863](#)] [[INSPIRE](#)].
- [21] M. Ciuchini, E. Franco, G. Martinelli and L. Reina, *ϵ'/ϵ at the Next-to-leading order in QCD and QED*, *Phys. Lett. B* **301** (1993) 263 [[hep-ph/9212203](#)] [[INSPIRE](#)].
- [22] T. Huber, E. Lunghi, M. Misiak and D. Wyler, *Electromagnetic logarithms in $\bar{B} \rightarrow X_s l^+ l^-$* , *Nucl. Phys. B* **740** (2006) 105 [[hep-ph/0512066](#)] [[INSPIRE](#)].
- [23] A.J. Buras, *Asymptotic Freedom in Deep Inelastic Processes in the Leading Order and Beyond*, *Rev. Mod. Phys.* **52** (1980) 199 [[INSPIRE](#)].
- [24] G. Buchalla, A.J. Buras and M.E. Lautenbacher, *Weak decays beyond leading logarithms*, *Rev. Mod. Phys.* **68** (1996) 1125 [[hep-ph/9512380](#)] [[INSPIRE](#)].
- [25] D.H. Adams and W. Lee, *Renormalization group evolution for the $\Delta S = 1$ effective Hamiltonian with $N(f) = 2 + 1$* , *Phys. Rev. D* **75** (2007) 074502 [[hep-lat/0701014](#)] [[INSPIRE](#)].
- [26] M. Gorbahn and U. Haisch, *Effective Hamiltonian for non-leptonic $|\Delta F| = 1$ decays at NNLO in QCD*, *Nucl. Phys. B* **713** (2005) 291 [[hep-ph/0411071](#)] [[INSPIRE](#)].
- [27] A. Lenz, U. Nierste and G. Ostermaier, *Penguin diagrams, charmless B decays and the missing charm puzzle*, *Phys. Rev. D* **56** (1997) 7228 [[hep-ph/9706501](#)] [[INSPIRE](#)].
- [28] S. Herrlich and U. Nierste, *Evanescent operators, scheme dependences and double insertions*, *Nucl. Phys. B* **455** (1995) 39 [[hep-ph/9412375](#)] [[INSPIRE](#)].
- [29] PARTICLE DATA GROUP collaboration, K.A. Olive et al., *Review of Particle Physics*, *Chin. Phys. C* **38** (2014) 090001 [[INSPIRE](#)].
- [30] K.G. Chetyrkin, J.H. Kuhn and M. Steinhauser, *RunDec: A Mathematica package for running and decoupling of the strong coupling and quark masses*, *Comput. Phys. Commun.* **133** (2000) 43 [[hep-ph/0004189](#)] [[INSPIRE](#)].
- [31] J. Charles et al., *Current status of the Standard Model CKM fit and constraints on $\Delta F = 2$ New Physics*, *Phys. Rev. D* **91** (2015) 073007 [[arXiv:1501.05013](#)] [[INSPIRE](#)] and online updates on <http://ckmfitter.in2p3.fr>.
- [32] S. Aoki et al., *Review of lattice results concerning low-energy particle physics*, *Eur. Phys. J. C* **74** (2014) 2890 [[arXiv:1310.8555](#)] [[INSPIRE](#)].
- [33] S. Gardner and G. Valencia, *The Impact of $|\Delta I| = 5/2$ transitions in $K \rightarrow \pi\pi$ decays*, *Phys. Rev. D* **62** (2000) 094024 [[hep-ph/0006240](#)] [[INSPIRE](#)].
- [34] V. Cirigliano, J.F. Donoghue and E. Golowich, *$K \rightarrow \pi\pi$ phenomenology in the presence of electromagnetism*, *Eur. Phys. J. C* **18** (2000) 83 [[hep-ph/0008290](#)] [[INSPIRE](#)].
- [35] S. Alekhin, A. Djouadi and S. Moch, *The top quark and Higgs boson masses and the stability of the electroweak vacuum*, *Phys. Lett. B* **716** (2012) 214 [[arXiv:1207.0980](#)] [[INSPIRE](#)].

- [36] L.K. Gibbons et al., *Measurement of the CP-violation parameter $\text{Re}(\epsilon'/\epsilon)$* , *Phys. Rev. Lett.* **70** (1993) 1203 [[INSPIRE](#)].
- [37] NA31 collaboration, G.D. Barr et al., *A New measurement of direct CP-violation in the neutral kaon system*, *Phys. Lett. B* **317** (1993) 233 [[INSPIRE](#)].
- [38] KTeV collaboration, A. Alavi-Harati et al., *Observation of direct CP-violation in $K_{S,L} \rightarrow \pi\pi$ decays*, *Phys. Rev. Lett.* **83** (1999) 22 [[hep-ex/9905060](#)] [[INSPIRE](#)].
- [39] NA48 collaboration, V. Fanti et al., *A New measurement of direct CP-violation in two pion decays of the neutral kaon*, *Phys. Lett. B* **465** (1999) 335 [[hep-ex/9909022](#)] [[INSPIRE](#)].
- [40] NA48 collaboration, J.R. Batley et al., *A Precision measurement of direct CP-violation in the decay of neutral kaons into two pions*, *Phys. Lett. B* **544** (2002) 97 [[hep-ex/0208009](#)] [[INSPIRE](#)].
- [41] KTeV collaboration, E. Abouzaid et al., *Precise Measurements of Direct CP-violation, CPT Symmetry and Other Parameters in the Neutral Kaon System*, *Phys. Rev. D* **83** (2011) 092001 [[arXiv:1011.0127](#)] [[INSPIRE](#)].
- [42] A.J. Buras and J.M. Gérard, *Isospin Breaking Contributions to ϵ'/ϵ* , *Phys. Lett. B* **192** (1987) 156 [[INSPIRE](#)].
- [43] W.A. Bardeen, A.J. Buras and J.M. Gérard, *The $K \rightarrow \pi\pi$ Decays in the Large- N Limit: Quark Evolution*, *Nucl. Phys. B* **293** (1987) 787 [[INSPIRE](#)].
- [44] W.A. Bardeen, A.J. Buras and J.M. Gérard, *A Consistent Analysis of the $\Delta I = 1/2$ Rule for K Decays*, *Phys. Lett. B* **192** (1987) 138 [[INSPIRE](#)].
- [45] A.J. Buras, J.-M. Gérard and W.A. Bardeen, *Large- N Approach to Kaon Decays and Mixing 28 Years Later: $\Delta I = 1/2$ Rule, \hat{B}_K and ΔM_K* , *Eur. Phys. J. C* **74** (2014) 2871 [[arXiv:1401.1385](#)] [[INSPIRE](#)].
- [46] A.J. Buras and J.M. Gérard, *Upper bounds on ϵ'/ϵ parameters $B_6^{(1/2)}$ and $B_8^{(3/2)}$ from large- N QCD and other news*, *JHEP* **12** (2015) 008 [[arXiv:1507.06326](#)] [[INSPIRE](#)].
- [47] A.J. Buras and J.M. Gérard, *Final State Interactions in $K \rightarrow \pi\pi$ Decays: $\Delta I = 1/2$ Rule vs. ϵ'/ϵ* , [arXiv:1603.05686](#) [[INSPIRE](#)].
- [48] E. Pallante and A. Pich, *Strong enhancement of ϵ'/ϵ through final state interactions*, *Phys. Rev. Lett.* **84** (2000) 2568 [[hep-ph/9911233](#)] [[INSPIRE](#)].
- [49] L. Lellouch and M. Lüscher, *Weak transition matrix elements from finite volume correlation functions*, *Commun. Math. Phys.* **219** (2001) 31 [[hep-lat/0003023](#)] [[INSPIRE](#)].
- [50] M. Constantinou et al., *$K \rightarrow \pi$ matrix elements of the chromagnetic operator on the lattice*, *PoS(LATTICE2014)390* [[arXiv:1412.1351](#)] [[INSPIRE](#)].
- [51] S. Bertolini, M. Fabbrichesi and E. Gabrielli, *The Relevance of the dipole Penguin operators in ϵ'/ϵ* , *Phys. Lett. B* **327** (1994) 136 [[hep-ph/9312266](#)] [[INSPIRE](#)].
- [52] N.G. Deshpande, X.-G. He and S. Pakvasa, *Gluon dipole penguin contributions to ϵ'/ϵ and CP-violation in hyperon decays in the Standard Model*, *Phys. Lett. B* **326** (1994) 307 [[hep-ph/9401330](#)] [[INSPIRE](#)].
- [53] S. Bertolini, J.O. Eeg and M. Fabbrichesi, *Studying ϵ'/ϵ in the chiral quark model: γ_5 -scheme independence and NLO hadronic matrix elements*, *Nucl. Phys. B* **449** (1995) 197 [[hep-ph/9409437](#)] [[INSPIRE](#)].

- [54] R. Barbieri, R. Contino and A. Strumia, ϵ' from supersymmetry with nonuniversal A terms?, *Nucl. Phys. B* **578** (2000) 153 [[hep-ph/9908255](#)] [[INSPIRE](#)].
- [55] A.J. Buras, G. Colangelo, G. Isidori, A. Romanino and L. Silvestrini, Connections between ϵ'/ϵ and rare kaon decays in supersymmetry, *Nucl. Phys. B* **566** (2000) 3 [[hep-ph/9908371](#)] [[INSPIRE](#)].
- [56] A.J. Buras, F. De Fazio and J. Girrbach, $\Delta I = 1/2$ rule, ϵ'/ϵ and $K \rightarrow \pi\nu\bar{\nu}$ in $Z'(Z)$ and G' models with FCNC quark couplings, *Eur. Phys. J. C* **74** (2014) 2950 [[arXiv:1404.3824](#)] [[INSPIRE](#)].
- [57] A.J. Buras, D. Buttazzo and R. Kneijens, $K \rightarrow \pi\nu\bar{\nu}$ and ϵ'/ϵ in simplified new physics models, *JHEP* **11** (2015) 166 [[arXiv:1507.08672](#)] [[INSPIRE](#)].
- [58] A.J. Buras, New physics patterns in ϵ'/ϵ and ϵ_K with implications for rare kaon decays and ΔM_K , *JHEP* **04** (2016) 071 [[arXiv:1601.00005](#)] [[INSPIRE](#)].
- [59] A.J. Buras, F. De Fazio and J. Girrbach-Noe, $Z - Z'$ mixing and Z -mediated FCNCs in $SU(3)_C \times SU(3)_L \times U(1)_X$ models, *JHEP* **08** (2014) 039 [[arXiv:1405.3850](#)] [[INSPIRE](#)].
- [60] A.J. Buras and F. De Fazio, ϵ'/ϵ in 331 Models, *JHEP* **03** (2016) 010 [[arXiv:1512.02869](#)] [[INSPIRE](#)].
- [61] A.J. Buras and F. De Fazio, 331 Models Facing the Tensions in $\Delta F = 2$ Processes with the Impact on ϵ'/ϵ , $B_s \rightarrow \mu^+\mu^-$ and $B \rightarrow K^*\mu^+\mu^-$, *JHEP* **08** (2016) 115 [[arXiv:1604.02344](#)] [[INSPIRE](#)].
- [62] M. Blanke, A.J. Buras and S. Recksiegel, Quark flavour observables in the Littlest Higgs model with T -parity after LHC Run 1, *Eur. Phys. J. C* **76** (2016) 182 [[arXiv:1507.06316](#)] [[INSPIRE](#)].
- [63] F. Goertz, J.F. Kamenik, A. Katz and M. Nardecchia, Indirect Constraints on the Scalar Di-Photon Resonance at the LHC, *JHEP* **05** (2016) 187 [[arXiv:1512.08500](#)] [[INSPIRE](#)].
- [64] M. Tanimoto and K. Yamamoto, Probing the SUSY with 10 TeV stop mass in rare decays and CP-violation of Kaon, [arXiv:1603.07960](#) [[INSPIRE](#)].
- [65] T. Kitahara, U. Nierste and P. Tremper, Supersymmetric Explanation of CP-violation in $K \rightarrow \pi\pi$ Decays, *Phys. Rev. Lett.* **117** (2016) 091802 [[arXiv:1604.07400](#)] [[INSPIRE](#)].